

Washington University in St. Louis

Washington University Open Scholarship

McKelvey School of Engineering Theses & Dissertations

McKelvey School of Engineering

Summer 8-14-2020

A Thesis on the Interactions between Lead Pipe Scales and Dissolved Silica from the Addition of Sodium Silicate as a Corrosion Inhibitor

Ziqi Wang

Washington University in St. Louis

Follow this and additional works at: https://openscholarship.wustl.edu/eng_etds



Part of the [Engineering Commons](#)

Recommended Citation

Wang, Ziqi, "A Thesis on the Interactions between Lead Pipe Scales and Dissolved Silica from the Addition of Sodium Silicate as a Corrosion Inhibitor" (2020). *McKelvey School of Engineering Theses & Dissertations*. 687.

https://openscholarship.wustl.edu/eng_etds/687

This Thesis is brought to you for free and open access by the McKelvey School of Engineering at Washington University Open Scholarship. It has been accepted for inclusion in McKelvey School of Engineering Theses & Dissertations by an authorized administrator of Washington University Open Scholarship. For more information, please contact digital@wumail.wustl.edu.

WASHINGTON UNIVERSITY IN ST. LOUIS
School of Engineering
Department of Energy, Environmental, and Chemical Engineering

Thesis Examination Committee:

Dr. Daniel Giammar, Chair

Dr. Young-Shin Jun

Dr. Kimberly Parker

A THESIS ON THE INTERACTIONS BETWEEN LEAD PIPE SCALES
AND DISSOLVED SILICA FROM THE ADDITION OF SODIUM SILICATE
AS A CORROSION INHIBITOR

by

Ziqi Wang

A thesis presented to the School of Engineering
of Washington University in partial fulfillment of the
requirements for the degree of
MASTER OF SCIENCE

May 2020

Saint Louis, Missouri

Abstract

A Thesis on the Interactions between Lead Pipe Scales and Dissolved Silica
from the Addition of Sodium Silicate as a Corrosion Inhibitor

by

Ziqi Wang

Master of Science in Chemical Engineering

Washington University in St. Louis, 2020

Research Advisor: Dr. Daniel Giammar

Ingestion of lead-contaminated drinking water is one of the major pathways for human exposure to lead. Addition of sodium silicate can potentially control lead release from lead service lines (LSLs) to the water that they convey, but the mechanism of silica uptake and corrosion control have not been reported. Knowledge of variables which affect the uptake of dissolved silica and the consumption rate of added sodium silicate by scales of corrosion products that are present on lead service lines will be useful to water utilities and distribution systems. This study investigated the effects of pH, initial silica concentration and mass of scales on the rates and extents of silica uptake by real scales removed from lead service lines and by hydrocerussite, which is one of the dominant lead-containing solids found in such scales. The study used batch experiments with these solid phases at environmentally relevant water chemistry conditions. Statistic models were built for different conditions to fit experimental data, a biphasic model was found to fit the data well.

Adsorption is a potential process of silica uptake, and adsorption isotherms were plotted in this study to observe the behavior of hydrocerussite and Buffalo scales during the uptake of dissolved silica. Other processes and possible reactions were also hypothesized to evaluate their role in the uptake of silica.

Acknowledgements

I would like to express my appreciation to all those who have supported me as I pursued my Masters' degree. First, I would like to acknowledge Washington University in St. Louis and the Department of Energy, Environmental and Chemical Engineering which provided me with the opportunity to receive a graduate education and conduct research in a field that is of interest to me. Studying here was an invaluable experience which taught me to be strong, be patient and have integrity in myself.

I wish to thank my advisor Prof. Giammar for providing assistance as I worked on my thesis, for teaching me how to do research on water treatment and environmental engineering, and for always being kind and patient during every individual meeting where I learned a lot. Thank you to committee, Dr. Jun and Dr. Parker, who took the time to review this thesis and attend my thesis defense. Thank you to all who worked in the Aquatic Chemistry Lab, particularly Anushka, who first led me to the laboratory during my independent study, told me about every details in the group and ran XRD and ICP-MS samples for me. I would also like to thank Weiyi for placing orders of the materials I used and Neha for doing BET analysis for me. I am also grateful to all the other group members, Yeunook, Anshuman, Yao, Kyle and Guiwei, for giving me suggestions and setting examples for me.

To all my friends and family who have seen and heard little of me over the past six years, thank you for your support and patience. At last, I want to thank a special person who is on the other side of the earth. She is always supporting me and makes me feel like she is always beside me, strengthens me and wakes me up when I am tired. Thank you Wenqing.

Ziqi Wang

Washington University in St. Louis

May 2020

Contents

Abstract	ii
Acknowledgements	iii
List of Tables	vi
List of Figures	viii
1. Introduction and Background	1
1.1 Past Lead Corrosion Research	2
1.2 Research about Sodium Silicate as a Corrosion Inhibitor	2
1.3 Research about Uptake of Dissolved Silica by Minerals	4
1.4 Introduction of Research in this Thesis	5
1.5 Predicted Equilibrium Concentrations of Dissolved Lead and Aluminum.....	6
2. Materials and Methods	9
2.1 Experimental Setup	9
2.1.1 Preparation and Source of Materials.....	9
2.1.1.1 Buffalo Scales.....	9
2.1.1.2 Soluble Sodium Silicate Solution	10
2.1.2 Batch Reactor Design	10
2.1.2.1 Experiments with Pure Hydrocerussite	10
2.1.2.2 Experiments with the Scales.....	13
2.1.3 Mass Balance	17
2.1.4 Experimental Timeline	17
2.2 Analytical Methods	19
2.2.1 Dissolved Metal Concentrations (Lead and Aluminum)	19
2.2.2 pH.....	20
2.2.3 Silica Concentration	20
2.2.4 BET Specific Surface Area Analysis.....	21
2.2.5 X-Ray Diffraction Analysis	21
2.2.6 Acid Digestion of Buffalo Scales	21
2.3 Statistical Analysis	21
3. Results and Discussion	22
3.1 Adsorption of Silica on Hydrocerussite (at pH 8.8).....	22

3.1.1 Characterization of Hydrocerussite Used in the Experiments.....	22
3.1.1.1 XRD Analysis.....	22
3.1.1.2 BET Specific Surface Area Analysis	23
3.1.2 Change in pH with Time.....	24
3.1.3 Adsorption Experiments on Hydrocerussite	24
3.1.3.1 Adsorption Isotherm and Sorption Site Density at pH 8.8.....	24
3.1.3.2 Silica Uptake Kinetics.....	26
3.1.4 Change of Lead Concentration with Time	33
3.2 Adsorption of Silica on Scales Removed from Lead Service Lines from Buffalo.....	34
3.2.1 Characterization of Scales Used in the Experiments	34
3.2.1.1 XRD Analysis.....	34
3.2.1.2 Acid Digestion of Scales	35
3.2.1.3 BET Specific Surface Area Analysis	36
3.2.2 Change in pH with Time.....	36
3.2.3 Mechanism of silica uptake.....	37
3.2.4 Change of Lead and Aluminum Concentration with Time	49
4. Conclusions and Recommendations for Future Work.....	53
4.1 Conclusions.....	53
4.2 Recommendations for Future Work	54
4.2.1 Suggestions for Experiments.....	54
4.2.2 Suggestions for Improvements of Modeling.....	55
References	56
Appendices	59
A. The Constants Used in the Calculation of Aquatic Chemistry.....	59
B. The Calculation of Solubility Curves	60
C. Calibration Curves Used in the Experiments	61
D. Source and Purity of Chemicals and Reagents Used in the Experiments	62
E. Additional Experimental Data.....	63

List of Tables

Table 1-1: Silicate equilibria (at 25°C)	3
Table 2-1: Water chemistry of prepared water in the experiments of silica uptake by pure hydrocerussite	11
Table 2-2: Sampling time and contents of each reactor in one set of experiments with pure hydrocerussite	12
Table 2-3: Chosen values of variables (pH, mass of hydrocerussite and initial silica concentration) in each set of experiments with pure hydrocerussite.....	13
Table 2-4: Water chemistry of prepared water in the experiments of silica uptake by scales, pH is 7.7 after the preparation (10 L of water)	14
Table 2-5: Comparison of synthesized Buffalo water and real Buffalo water	14
Table 2-6: Sampling time and contents of each reactor in one set of experiments with scales	16
Table 2-7: Chosen values of variables (pH, mass of hydrocerussite and initial silica concentration) in each set of experiments with scales (the highlighted row of experiment was planned but not finished).....	17
Table 2-8: Sampling time of reactors in one set of experiments with pure hydrocerussite	18
Table 2-9: Sampling time of reactors in one set of experiments with scales.....	19
Table 2-10: Reagents used in colorimetric method for measurement of dissolved monomeric silica.....	20
Table 3-1: Comparison of equilibrium concentration (with 0.1 g hydrocerussite in 100 mL solution) and final silica concentration in control experiments with no hydrocerussite in experiments 3, 14, 15 and 16 (Table 2-3).....	27
Table 3-2: Average removal of dissolved silica in experiments 1-6 (Table 2-3) with 20 mg/L silica was added.....	28
Table 3-3: Constants used in modeling the uptake rate of silica by hydrocerussite (the model is using g/L as the units for the amount of hydrocerussite, but the uptake is actually controlled by the surface area which is linearly proportional to the mass)	29
Table 3-4: Constants used in the biphasic modeling equation.....	31
Table 3-5: Average removal of dissolved silica for different initial silica concentrations at pH 8.8 and difference of final silica concentration in control experiments with no scales from initial silica concentration in experiments 5 and 6 (Table 2-7)	39
Table 3-6: Average removal of dissolved silica for different initial silica concentrations at pH 7.7 and difference of final silica concentration in control experiments with no scales from initial silica concentration in experiments 1 and 4 (Table 2-7)	40

Table 3-7: Average removal of dissolved silica at pH 7.7 and 8.8 and difference of final silica concentration in control experiments with no scales from initial silica concentration in experiments 4 and 5 (Table 2-7) (initial silica concentration = 9 mg/L, scale amount = 0.1 g)	41
Table 3-7: Silica removal by different amounts of silica at pH 8.8 in experiments 2, 3 and 6 (Table 2-7) with initial silica concentration = 20 mg/L	43
Table 3-8: Silica removal by different amounts of silica at pH 7.7 in experiments 1 and 7 (Table 2-7) with initial silica concentration = 20 mg/L	44
Table 3-9: Constants used in the modeling equation (the model is using g/L as the unit of amount of hydrocerussite, but the uptake is actually controlled by the surface area which is linearly proportional to the mass)	45
Table 3-10: Constants used in the biphasic modeling equation	48
Table S1. Chemical formulas and acidity constants at 25°C of some important acids	59
Table S2. Stability constants for some Al-ligand and Pb-ligand complexes. Values correspond to $\log\beta$ for formation of the complex.	59
Table S3. The K_{s0} value of some solids of interest	59
Table S4. Standard silica concentration calibration	62
Table S5. Chemicals and reagents in the experiments	62

List of Figures

Figure 1-1: Species in equilibrium with amorphous silica (diagram computed with equilibrium constants at 25°C given in Table 1-1)	3
Figure 1-2: Dissolved lead concentration (cerussite and hydrocerussite equilibrate with water with dissolved inorganic carbon (DIC) of 24 mg/L as C at pH 6~10).....	7
Figure 1-3: Dissolved aluminum concentration (amorphous aluminum hydroxide and gibbsite equilibrate with water with dissolved inorganic carbon (DIC) of 24 mg/L as C).....	7
Figure 2-1: Pipes sections with scales (left 1&2), pipe sections after scales were scraped off (right 1&2)	9
Figure 2-2: Procured scales after being ground	10
Figure 2-3: Reactor of batch experiments with pure hydrocerussite	11
Figure 2-4: Reactor of batch experiments with Buffalo scales	14
Figure 3-1: Comparison of purchased hydrocerussite and the reference patterns of hydrocerussite and two other solids that appear to be present in this material (the experimental and reference patterns have been scaled so that the intensities of their highest peaks are the same).....	23
Figure 3-2: pH variation with time (with 0.2 g of hydrocerussite, 20 mg/L silica in 100 mL of solution).....	24
Figure 3-3: Adsorption isotherm of silica on hydrocerussite at pH 8.8 for 96-hour equilibration time.....	25
Figure 3-4: Variation in dissolved silica concentration with time for different initial silica concentrations with 0.1 g hydrocerussite in the reactor (in 100 mL of water, which makes the concentration of hydrocerussite 1 g/L) in experiments 3, 14, 15 and 16 (Table 2-3). Error bars are showing 1 standard deviation. The initial concentrations of silica in the series labeled 20, 40 and 50 mg/L case were not exactly 20, 40 and 50 because of an experimental error (<5%) in the addition of solutions to prepare the reactors.....	28
Figure 3-5: Experimental data (experiments 1-6 in Table 2-3) compared with model output (initial silica concentration is 0.35 mmol/L= 20 mg/L).....	30
Figure 3-6: Experimental data (experiments 1-6 in Table 2-3) compared with biphasic model at pH 8.8 (initial silica concentration is 0.35 mmol/L=20 mg/L).....	32
Figure 3-7: Experimental data (experiments 3, 14, 15, 16 in Table 2-3) compared with biphasic model at pH 8.8 (concentration of hydrocerussite in the reactors is 1 g/L)	33
Figure 3-8: Variation in dissolved lead concentration with time (with 0.2 g of hydrocerussite and 20 mg/L silica in 100 mL of water at pH 8.8) the yellow point and orange point are overlapping with each other	34

Figure 3-9: XRD comparison of procured Buffalo scales and the standard pattern of hydrocerussite (the experimental and reference patterns have been scaled so that the intensities of their highest peaks are the same)	35
Figure 3-10: pH variation with time with an initial pH of 8.8 (with 0.1 g of scales and 20 mg/L silica in 50 mL of solution).....	36
Figure 3-11: pH variation with time with an initial pH of 7.7 (with 0.1 g of scales and 20 mg/L silica in 50 mL of solution).....	37
Figure 3-12: Silica concentration variation with time for different silica initial concentrations in experiments 5 and 6 (Table 2-7) (with 0.1 g of scales in 50 mL of solution at pH 8.8), duplicates are performed for this experiment.....	39
Figure 3-13: Silica concentration variation with time for different silica initial concentrations in experiments 1 and 4 (Table 2-7) (with 0.1 g of scales in 50 mL of solution at pH 7.7), duplicates are performed for this experiment.....	40
Figure 3-14: Silica concentration variation with time for different pH values in experiments 4 and 5 (Table 2-7) (initial silica concentration = 9 mg/L, scale amount = 0.1 g), duplicates are performed for this experiment.....	41
Figure 3-15a: Comparison of adsorption isotherm of silica on hydrocerussite and scales at pH 8.8 for 96-hour equilibration time (unit of sorption density $\mu\text{mol/g}$).....	42
Figure 3-15b: Comparison of adsorption isotherm of silica on hydrocerussite and scales at pH 8.8 for 96-hour equilibration time (unit of sorption density $\mu\text{mol/m}^2$).....	42
Figure 3-16: Silica concentration variation with time for different amounts of scales in experiments 2, 3 and 6 (Table 2-7) (initial silica concentration = 20 mg/L, pH = 8.8), duplicates are performed for this experiment.	43
Figure 3-17: Silica concentration variation with time for different amounts of scales in experiments 1 and 7 (Table 2-7) (initial silica concentration = 20 mg/L, pH = 7.7), duplicates are performed for this experiment.	44
Figure 3-18: Experimental data compared with built model at pH 7.7 in experiments 1 and 7 (Table 2-7) (initial silica concentration is 0.35 mmol/L=20 mg/L).....	46
Figure 3-19: Experimental data compared with built model at pH 8.8 in experiments 2, 3 and 6 (Table 2-7) (initial silica concentration is 0.35 mmol/L=20 mg/L).....	47
Figure 3-20: Experimental data compared with biphasic model at pH 7.7 in experiments 1 and 7 (Table 2-7) (initial silica concentration is 0.35 mmol/L=20 mg/L).....	48
Figure 3-21: Experimental data compared with biphasic model at pH 8.8 in experiments 2, 3 and 6 (Table 2-7) (initial silica concentration is 0.35 mmol/L=20 mg/L).....	49
Figure 3-22: Lead and aluminum concentration variation with time at pH 7.7 (with 0.1 g scales and 20 mg/L silica in 50 mL of solution)	51
Figure 3-23: Lead and aluminum concentration variation with time at pH 8.8 (with 0.1 g scales and 20 mg/L silica in 50 mL of solution)	52

Figure S1. Calibration curve of silica (UV-Vis wavelength $\lambda=410$ nm)..... 61
Figure S2. Silica concentration variation with time for different amounts of hydrocerussite (in 100 mL of water, initial silica concentration 20 mg/L, pH 8.8)..... 63

Chapter 1

Introduction and Background

Lead had been used as the material for service lines that supply water to homes for around a hundred years in the United States. Over time corrosion scales form on the inner surfaces of these pipes that are comprised of solid Pb(II) and Pb(IV) solids. These solids include cerussite (PbCO_3), hydrocerussite ($\text{Pb}_3(\text{CO}_3)_2(\text{OH})_2$), litharge (PbO) and plattnerite (PbO_2) can form. According to the solubility of hydrocerussite and cerussite, dissolved lead concentrations in water in contact with pipes with scales composed of these lead carbonates can be present at levels that are concerns for human health.

Lead can cause severe damage to the brain and kidneys and, ultimately, death. By mimicking calcium, lead can cross the blood–brain barrier. It degrades the myelin sheaths of neurons, reduces their numbers, interferes with neurotransmission routes, and decreases neuronal growth.^[1] In the Guidelines for Drinking-Water Quality established by the World Health Organization, the provisional guideline value is set at 10 $\mu\text{g/L}$ on the basis of treatment performance and analytical achievability.^[2]

In 1991, the Lead and Copper Rule set an action level of 15 $\mu\text{g/L}$ for lead to regulate the concentration of lead in the tap water, which means the system must undertake additional actions to control corrosion when lead concentrations exceed the action level at 10% of monitored customer taps.^[3] Recently, the EPA has proposed a revised version of the Lead and Copper Rule that would introduce a trigger level of 10 $\mu\text{g/L}$ that requires more proactive planning in communities with lead service lines (LSLs).^[4] To reduce the release of lead, there are two main methods: (1) controlling pH and alkalinity and (2) using corrosion inhibitors. The key difference between these two methods is the mechanism of corrosion control. Controlling pH or alkalinity is taking advantage of the low solubility of Pb(II) carbonates at pH 8~9, while the corrosion inhibitors can chemically combine with lead in the pipes to convert it into less soluble substances or to form a layer preventing the lead from being released into water.^[5]

1.1 Past Lead Corrosion Research

Research about lead corrosion control can be dated to the beginning of the last century.^[6] People found that lead release from lead pipes is influenced by stagnation time^[7], flow velocity, and water chemistry, which is revealed by experiments in the laboratory. Schock pointed out that lead concentrations rarely reach equilibrium in lead service lines (LSLs) because of the short stagnation time in pipes with flowing water.^[8] Also, flow velocity can influence lead release in several ways. First, flow velocity can affect erosion mechanisms of corrosion products and the formation of pipe scales.^[9] Second, increase in flow velocity can make lead-containing solid particles detach from pipe scales and contribute to total lead concentration.^[10] Third, flow rate can affect mass transfer rate of lead release from the pipe scales to the water, because slowly flowing water near scales may be more concentrated with dissolved lead.^[11]

1.2 Research about Sodium Silicate as a Corrosion Inhibitor

In addition to the adjustment of alkalinity and pH, corrosion inhibitors such as phosphate or silicate can be used as an alternative for corrosion control treatment as per the guidelines in the LCR Guidance Manual published by EPA.^[12]

As a common element in nature, silicon is ubiquitous in soils and natural waters. When present as dissolved species in water, silicon is referred to as dissolved silica (SiO_2). The solubility characteristics of amorphous silica can be explained by its dissociation into monomeric and simple multimeric silicates. Monomeric species are orthosilicic acid (H_4SiO_4) and its two deprotonated forms (H_3SiO_4^- and $\text{H}_2\text{SiO}_4^{2-}$). Multimeric species like polymeric silicates form in an oversaturated solution of amorphous silica. The solubility of amorphous silica for the entire pH range can be obtained using dissociation constants of H_4SiO_4 .^[13]

Table 1-1: Silicate equilibria (at 25°C)

Reactions	logK
$\text{SiO}_2(\text{amorph}) + 2\text{H}_2\text{O} = \text{H}_4\text{SiO}_4$	-2.7
$\text{H}_4\text{SiO}_4 = \text{H}_3\text{SiO}_4^- + \text{H}^+$	-9.46
$\text{H}_3\text{SiO}_4^- = \text{H}_2\text{SiO}_4^{2-} + \text{H}^+$	-12.56
$4\text{H}_4\text{SiO}_4 = \text{Si}_4\text{O}_6(\text{OH})_6^{2-} + 2\text{H}^+ + 4\text{H}_2\text{O}$	-12.57

Therefore, the silicate equilibria can be computed using the following equation:

$$\text{TOTSiO}_2 = \text{H}_4\text{SiO}_4 + \text{H}_3\text{SiO}_4^- + \text{H}_2\text{SiO}_4^{2-} + \text{Si}_4\text{O}_6(\text{OH})_6^{2-}$$

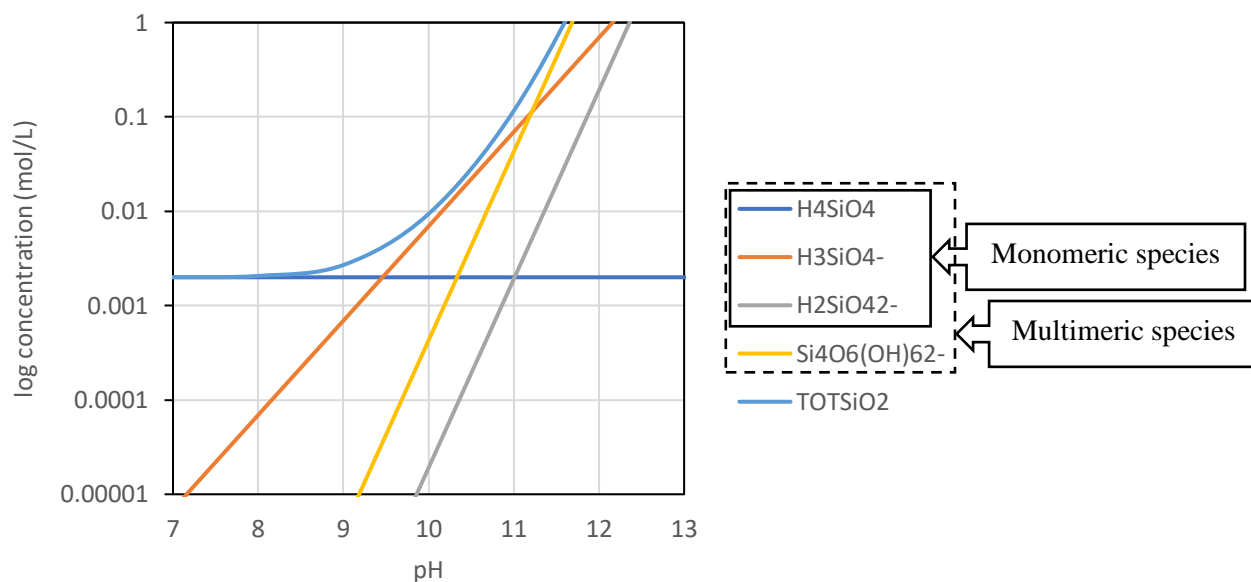


Figure 1-1: Species in equilibrium with amorphous silica (diagram computed with equilibrium constants at 25°C given in Table 1-1)

Corrosion control using sodium silicate has a long history. In 1922 Thresh reported that the alkali silicates are more effective than silicic acid to prevent lead dissolution.^[6] Then in 1924 Donal suggested the use of sodium silicate as an inhibitor in England.^[14] Thereafter, it was used for galvanized iron, galvanized steel, yellow brass and copper pipes.^[15] In 1951, by using sodium silicates in iron pipes with zinc and magnesium, Lehrman and Shuldener reported that the film formed on the pipe could be pictured as a two-layer deposit without a sharp line of demarcation. The lower layer consists of the initial metal corrosion products such as metal oxides and hydroxides. The upper layer is a conglomerate of an adsorbed

form of silica and the metal hydroxides enmeshed with silica gel, which had extracted compounds of iron, calcium and magnesium from water.^[16]

In 1956, Duffek and McKinney developed a novel method of studying corrosion inhibition of iron with sodium silicate that used polished steel electrodes pretreated with sodium silicates and sodium hydroxide for 24 or 48 hours to determine the effect of silicates on the corrosion of the steel. This proved that silicates were effective in controlling steel corrosion. No corrosion products were observed on electrodes treated with sodium silicate, while those with sodium hydroxide corroded.^[17]

Since 1980, the control of lead corrosion using dissolved silica has reached many achievements based on the findings of investigators before them. Although Sheiham^[18] mentioned that a 10 mg/L dose of silica had little effect on lead dissolution at pH 6.5, Michniewicz^[19] reported that 16 mg/L dose of silica successfully reduced lead concentration from 83 to 16 µg/L at pH 8.8. Furthermore, Schantz confirmed silica addition could reduce lead concentration and prevent lead dissolution at higher pH values (8~9) in loop study and field study.^[20] At the same time, there is a scarcity in literature that compares the role of sodium silicate and pH adjustment alone in controlling lead release.

1.3 Research about Uptake of Dissolved Silica by Minerals

In 2008, Luxton et al reported that dissolved silica is capable of inhibiting arsenite adsorption on goethite by competing for adsorption sites on goethite. They observed that silica could effectively compete with arsenate for adsorption to goethite.^[21] Also, low concentrations of silica resulted in minimal desorption of arsenite from goethite. Similarly, Maiti et al reported that the adsorption of arsenite and arsenate ions on laterite was reduced by up to about 17% in the presence of different concentrations of silica in the system.^[22] In 2000, Meng et al reported that the removal of arsenite and arsenate by coprecipitation with ferric chloride was significantly reduced by silica when its concentration was higher than 1 mg/L and pH was greater than 5. Two reasons were mentioned in their research, one is the reaction between silica and ferric hydroxide sites when H_2SiO_3 dissociates into

anions at higher pH values; the other reason is that soluble polymers and highly dispersed colloids are formed in the interaction between silica and Fe(III). They also mentioned that the silica removal increased when the surface potential decreased, which indicated that the chemical binding affinity of silica overcame the electrostatic repulsion between the anions and the charged surface.^[23]

In addition to adsorption, coprecipitation is a significant cause of the uptake of silica by minerals. In order to remove dissolved silica which can clog water pipes and reduce thermal efficiencies of boilers, Tokoro et al systematically studied the adsorption and coprecipitation of silica with aluminum hydroxide. They reported that more silica was removed by coprecipitation than by adsorption, and they also observed the formation of kaolinite $[\text{Al}_2\text{Si}_2\text{O}_5(\text{OH})_4]$ and boehmite $[\text{AlOOH}]$. Their time-based studies of residual silica concentrations indicated that silicate was removed in two steps: a rapid initial uptake and a slow uptake over the next several hours.^[24]

Based on previous studies, some minerals are capable of interacting with dissolved silica^{[23][24]}, which implies that there could be interactions between pipe scales and added sodium silicate. The nature of these interactions can be affected by pH since the pH affects the solubility and surface properties of the solid phases present as well as the speciation of the dissolved silica.

1.4 Introduction of Research in this Thesis

Some research had been pursued in this direction in our group. That research involved bench-scale experiments with varied doses of sodium silicate (weight ratio of 3.22) conducted with lead soldered copper pipes and with harvested lead pipes.^[5] Before the addition of sodium silicate as an inhibitor, both sets of pipes were conditioned with synthetic water receiving a low dose of 0.2 mg/L as PO_4^{3-} of blended phosphate. The harvested lead pipes were from Buffalo Water, a water utility with one of the Great Lakes as the source water. An artificial water chemistry was designed to match the pH, alkalinity, hardness, blended phosphate, and chlorine concentration type of that system. While new

lead soldered copper pipes were used in the pipe reactor experiments, lead service lines were harvested from a system that had been delivering water with pH of 7.7 and dissolved inorganic carbon (DIC) of 24 mg/L as C. As the released lead concentrations in the system measured every week became stable around a certain level, the addition of silica decreased the level of lead released. On an average about 3 mg/L out of 20 mg/L silica that was added was consumed in a week's time and the uptake of silica decreased from week to week. Based on the intriguing observations from the flow experiments with harvested lead pipes, this thesis research involved batch experiments that will focus on the uptake of dissolved silica by actual scales from lead pipes procured from Buffalo, New York and by the dominant crystalline phase (hydrocerussite) present in those scales.. This thesis aims to figure out how silica interacts with the actual scale and the statistic model of silica consumption in an attempt to understand the mechanism of lead release in the presence of silica. It is hypothesized that silica is adsorbed on to the scales resulting in a reduced silica concentration. Moreover, it is possible that silica can precipitate on the aluminum-enriched scales and convert into insoluble solids. Research can be divided into two parts: (1) uptake of dissolved silica by pure hydrocerussite which is one of the main components of the scales; and (2) uptake of dissolved silica by actual scales which contains both hydrocerussite and amorphous aluminum hydroxide.

1.5 Predicted Equilibrium Concentrations of Dissolved Lead and Aluminum

The solubility of a certain metal mainly depends on the pH and the water chemistry so that solubility curves are computed to assist the assessment of lead release control:

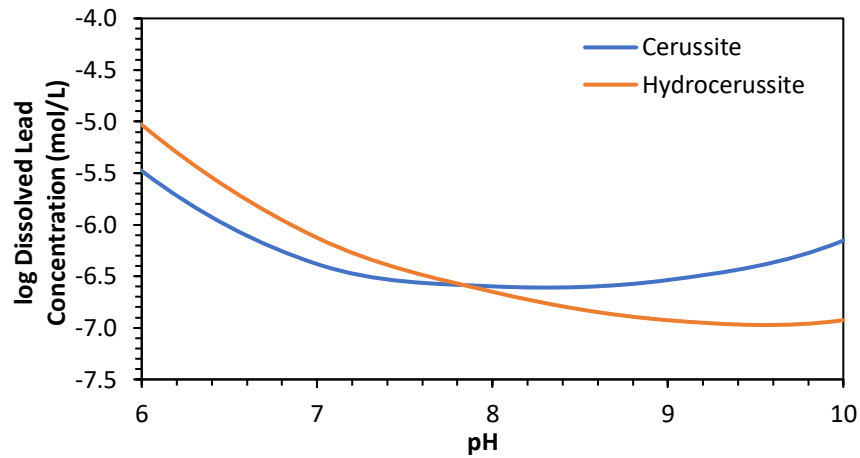


Figure 1-2: Dissolved lead concentration (cerussite and hydrocerussite equilibrate with water with dissolved inorganic carbon (DIC) of 24 mg/L as C at pH 6~10)

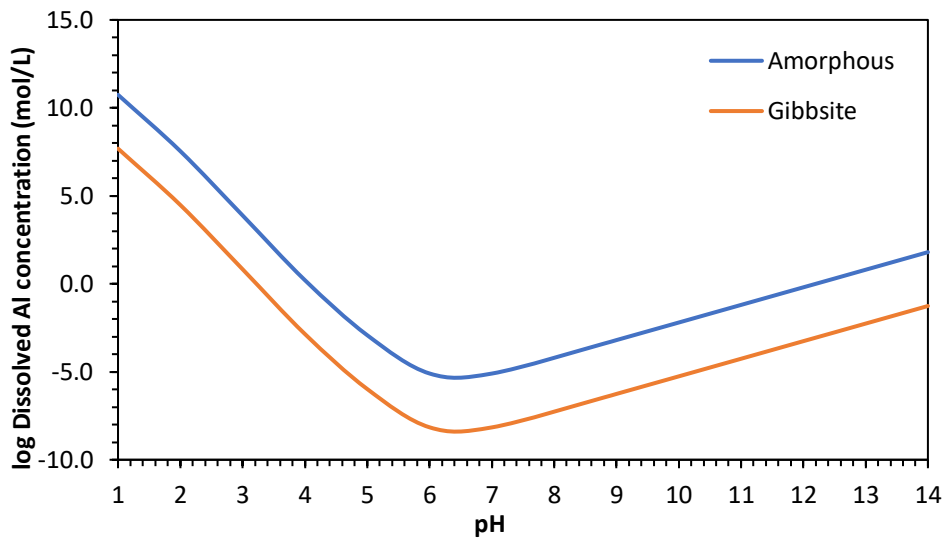


Figure 1-3: Dissolved aluminum concentration (amorphous aluminum hydroxide and gibbsite equilibrate with water with dissolved inorganic carbon (DIC) of 24 mg/L as C)

In the second chapter, methods and materials used in this thesis will be presented. In order to comprehend how different variables affect the uptake of silica in batch experiments, experiments are designed in a manner that one variable is manipulated at a time. In the third chapter, the findings of the experimental are summarized, and results will be interpreted from the discussion of two main parts of the experiments. The analysis considered the uptake of silica and the change in concentrations of lead and other metals. Multiple models

are used to fit the data to find the best fit. In the last chapter, the effect of silica in controlling lead release via batch experiments are discussed. Suggestions for future research directions are also provided.

Chapter 2

Materials and Methods

2.1 Experimental Setup

2.1.1 Preparation and Source of Materials

2.1.1.1 Buffalo Scales

The scales used in the experiments were removed from approximately 80-year-old lead pipes harvested by the utility Buffalo Water in Buffalo, New York. Buffalo Water treats and distributes water from Lake Erie, one of the Great Lakes, which has a composition similar that of other major cities supplied that have one of the Great Lakes as their water source (e.g., Chicago, Cleveland, Detroit, Milwaukee). Transverse sections of the pipe were cut out from a long pipe using a hack saw. Then scales were scraped off the from the inside of the pipe sections using a spatula. Procured scales from the entire length of the pipe were ground completely using an agate mortar and pestle, well mixed and stored in a closed container at room temperature.



Figure 2-1: Pipes sections with scales (left 1&2), pipe sections after scales were scraped off (right 1&2)



Figure 2-2: Procured scales after being ground

2.1.1.2 Soluble Sodium Silicate Solution

Liquid sodium silicate, also known as waterglass, is produced by melting high purity silica sand along with sodium carbonate at 1100-1200°C. The molten glass is combined with water resulting in a solution that may consist of 24-36 weight% SiO_2 with an $\text{SiO}_2/\text{Na}_2\text{O}$ weight ratio between 1.60 and 3.22. For water treatment applications, the $\text{SiO}_2/\text{Na}_2\text{O}$ ratio is usually 3.22.^[13] In this study, the sodium silicate solution ($\text{SiO}_2/\text{Na}_2\text{O}$ ratio is 3.22) used in the experiments was provided by PQ Corporation.

2.1.2 Batch Reactor Design

Batch experiments were carried out in closed containers. After the addition of solids and water with a specific composition (discussed in the next section), the contents of the containers became well-mixed suspensions. Then the containers were placed on a multiposition stir plate (VARIOMAG, Thermo, U.S.A.) and continuously stirred with polypropylene-coated magnetic stir bars at room temperature.

2.1.2.1 Experiments with Pure Hydrocerussite

The water chemistry of solutions used in the adsorption experiments with pure hydrocerussite was designed to be as simple as it could be as long as the pH value and dissolved inorganic carbon (DIC) was the same as Buffalo water as shown in Table 2-1. In

the adsorption experiments of silica on pure hydrocerussite, the pH value in the system was maintained at 8.8, the reason for choosing 8.8 is that after the addition of 20 mg/L silica, pH of Buffalo water will increase from 7.7 to 8.8 if that addition is not accompanied by any pH readjustment. In the adsorption experiments the pH was periodically measured and readjusted to pH 8.8 with either dilute HNO₃ or NaOH. The volume of reactors is 100 mL with a stir bar at a rotation speed of 700 rpm.

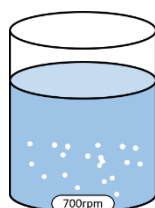


Figure 2-3: Reactor of batch experiments with pure hydrocerussite

Table 2-1: Water chemistry of prepared water in the experiments of silica uptake by pure hydrocerussite

Chemical	Stock concentration	Added volume (mL)	Concentration (mg/L)	Concentration (mmol/L)
NaHCO ₃	66 g/L	5.6	184.8	2.20
Na ₂ SiO ₃	20 g/L	2.0	20	0.83
HNO ₃	1% (10 g/L)	4.2	21	0.33

One set of experiments was setup initially to determine how much silica could be adsorbed on hydrocerussite and how long it would take for silica to reach adsorption equilibrium with hydrocerussite. Silica samples were stored at room temperature and were measured together at the end of each set of experiments. Duplicate or triplicate reactors were operated for each time point and the standard deviation will be shown in the plots in Chapter 3. The design for one set of experiments (14 sets of experiments in total) is shown below:

Table 2-2: Sampling time and contents of each reactor in one set of experiments with pure hydrocerussite

No.	Time (hour)	Mass of hydrocerussite (g)	Initial silica concentration (mg/L as SiO ₂)	pH	Volume (mL)
1	0.5	0.200	20	8.8	100
2	1	0.200	20	8.8	100
3	1.5	0.200	20	8.8	100
4	2	0.200	20	8.8	100
5	3	0.200	20	8.8	100
6	4	0.200	20	8.8	100
7	6	0.200	20	8.8	100
8	8	0.200	20	8.8	100
9	16	0.200	20	8.8	100
10	24	0.200	20	8.8	100
11	48	0.200	20	8.8	100
12	72	0.200	20	8.8	100
13	96	0.200	20	8.8	100
14	96	0.200	0	8.8	100
15	96	0.000	20	8.8	100
16	96	0.000	0	8.8	100

The experiment also included three control reactors. One control reactor with no sodium silicate was set to find the lead concentration in the system if there was no sodium silicate added, and a control reactor with no hydrocerussite was setup to find the change in dissolved silica throughout the entire duration of the experiment (if silica could be taken up even if hydrocerussite was not in the reactor). The last control reactor with synthesized water containing neither silica nor hydrocerussite was setup to exclude the effect of the containers or stir bars on silica concentration.

In the main experiments, the mass of hydrocerussite and initial silica concentrations were chosen as variables. In each set of experiments, one of these two variables was varied to investigate the effect of that variable on the uptake of silica and release of lead in the reactors. Silica was first added to a concentration of 20 mg/L of silica in the experiments because this concentration had already been applied in pipe loop experiments ^[14] to control lead release, and the mass of hydrocerussite was calculated based on the ratio of mass of

scales in real pipes to volume of water in the pipe (0.2 g/100 mL). Additional silica concentrations were then evaluated.

Table 2-3: Chosen values of variables (pH, mass of hydrocerussite and initial silica concentration) in each set of experiments with pure hydrocerussite

No.	Mass of hydrocerussite (g)	Initial silica concentration (mg/L as SiO ₂)	pH
1	0.200	20	8.8
2	0.150	20	8.8
3	0.100	20	8.8
4	0.075	20	8.8
5	0.050	20	8.8
6	0.025	20	8.8
7	0.150	10	8.8
8	0.075	10	8.8
9	0.025	10	8.8
10	0.150	5	8.8
11	0.075	5	8.8
12	0.025	5	8.8
13	0.100	0	8.8
14	0.100	30	8.8
15	0.100	40	8.8
16	0.100	50	8.8

Data points with different initial silica concentrations and different masses of hydrocerussite were collected to resolve the adsorption isotherm for adsorption of dissolved silica on hydrocerussite.

2.1.2.2 Experiments with the Scales

In the adsorption experiments of dissolved silica on Buffalo scales, the volume of reactors is 50 mL with a stir bar at a rotation speed of 500 rpm. Water chemistry of the baseline synthesized water was designed to be close to that of Buffalo water.

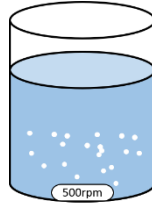


Figure 2-4: Reactor of batch experiments with Buffalo scales

Table 2-4: Water chemistry of prepared water in the experiments of silica uptake by scales, pH is 7.7 after the preparation (10 L of water)

Chemicals	Stock concentration (g/L)	Added volume (mL)	Actual concentration (mg/L)
NaHCO ₃	66	28	184.8
Ca(OH) ₂	1.4	10.2	1.428
CaCl ₂	350	5	175
NaF	3.78	0.1	0.0378
H ₂ SO ₄	49	1.65	8.085
Blended phosphate	3.9	2	0.78
Free chlorine	8.15	1	0.815
Na ₂ SiO ₃	0.4	0	0

Table 2-5: Comparison of synthesized Buffalo water and real Buffalo water

Species	Target range	Average of the range	Achieved	Units
Ca ²⁺	34 -50	46	48	mg/L
Na ⁺	11	11	44	mg/L
Ba ²⁺	0.02	0.02	-	mg/L
SO ₄ ²⁻	23	23	13.2	mg/L
NO ₃ ⁻	0.07 - 0.16	0.12	-	mg/L
F ⁻	0.12	0.12	0.12	mg/L
Free Chlorine	0.82 - 1.49	1.10	1.12	mg/L
Alkalinity	91 - 98	94	93	mg/L as CaCO ₃
pH	7.4 – 7.9	7.7	7.68	-
TDS	94 - 177	156	302	mg/L
Ca Hardness	84 - 126	116	121	mg/L as CaCO ₃
Orthophosphate	0.14 – 0.27	0.20	-	mg/L

In addition to the experiments done with scales in baseline water chemistry, some experiments were done at different pH and with different dissolved silica concentrations. Solutions needed to achieve different dissolved silica concentrations and different pH conditions were prepared separately from the original stock of synthesized water, they are 400 mg/L sodium silicate solution and 1% (10 g/L) nitric acid.

Initially, one set of experiments were setup to figure out the amount of dissolved silica that could be taken up by scales and the time for silica uptake to reach equilibrium. In another set of experiments, a pre-equilibrium stage was included before the addition of sodium silicate to see how dissolved lead concentrations would change during the initial immersion of the scales in the water and what effect silica addition would bring to the metal concentrations. Therefore, the scales and synthesized water without silica were combined and stirred for one day before the addition of silica and adjustment of pH to reach the needed concentration of silica and pH value. One control reactor with no silica was setup to find the lead concentration in the system if there was no sodium silicate addition, and another control reactor with no scales was set to find if silica could be taken up even if scale was not in the reactor. An additional control reactor with neither silica nor scales was set to exclude the effect of the containers or stir bars on silica concentration. One set of experiments (7 sets of experiments in total) is shown below:

Table 2-6: Sampling time and contents of each reactor in one set of experiments with scales

No.	Time	Mass of scales (g)	Initial silica concentration (mg/L as SiO ₂)	pH	Volume (mL)
1	-23.5 h	0.100	0	8.8	50
2	-23 h	0.100	0	8.8	50
3	-22 h	0.100	0	8.8	50
4	-20 h	0.100	0	8.8	50
5	-16 h	0.100	0	8.8	50
6	0 h	0.100	0	8.8	50
7	1 min	0.100	20	8.8	50
8	5 min	0.100	20	8.8	50
9	0.5 h	0.100	20	8.8	50
10	1 h	0.100	20	8.8	50
11	2 h	0.100	20	8.8	50
12	4 h	0.100	20	8.8	50
13	8 h	0.100	20	8.8	50
14	24 h	0.100	20	8.8	50
15	48 h	0.100	20	8.8	50
16	72 h	0.100	20	8.8	50
17	96 h	0.100	20	8.8	50
18	96 h	0.100	0	8.8	50
19	96 h	0.000	20	8.8	50
20	96 h	0.000	0	8.8	50

In these experiments, pH values, amounts of scales and initial dissolved silica concentrations were chosen as variables. In each set of experiments, one of the variables was varied to examine its effect on the uptake of silica and lead concentration in the reactors. A concentration of 20 mg/L silica was first studied in the experiments because this concentration had already been applied in pipe loop experiments ^[2] to control lead release, and the mass of scales was calculated based on the ratio of mass of scales in real pipes to volume of water in the pipe (0.1 g/50 mL).

Table 2-7: Chosen values of variables (pH, mass of hydrocerussite and initial silica concentration) in each set of experiments with scales (the highlighted row of experiment was planned but not finished)

No.	Mass of scales (g)	Initial silica concentration (mg/L as SiO ₂)	pH
1	0.100	20	7.7
2	0.050	20	8.8
3	0.025	20	8.8
4	0.100	10	7.7
5	0.100	10	8.8
6	0.100	20	8.8
7	0.050	20	7.7

Data points were collected and plotted to see how the silica concentrations changed in each set of experiments. Then statistical models were used to figure out the effect of the three variables on the uptake of silica. The adsorption isotherm for silica on hydrocerussite and scales was plotted as well.

2.1.3 Mass Balance

To determine the consumption of silica by reaction with the suspended solids in the reactor, the difference between the initial and final concentrations were calculated. The mass balance equation is:

$$[\textit{consumed silica}] = [\textit{added silica}] - [\textit{silica left}] \quad (1)$$

2.1.4 Experimental Timeline

In the adsorption experiments with silica on hydrocerussite, all the reactors were started at almost at the same time. The sampling time was chosen to plot a smooth curve of silica concentration, so when the silica concentration is decreasing fast, the intervals between two samples in the beginning is shorter to account for any rapid decrease in dissolved silica; when the silica concentration is reaching a plateau, the time between two samples was as long as 24 hours. The sampling in the control reactor was designed to take place at the same

time that a reactor from the main experiment was sampled such that each experimental data point had a supporting control data point.

Table 2-8: Sampling time of reactors in one set of experiments with pure hydrocerussite

Reaction time	Event
0.5 h	0.5-hour sample
1 h	1-hour sample
1.5	1.5-hour sample
2	2-hour sample
3	3-hour sample
4	4-hour sample
6	6-hour sample
8	8-hour sample
16	16-hour sample
24	24-hour sample
48	48-hour sample
72	72-hour sample
96	96-hour sample
96	No silica control
96	No hydrocerussite control
96	No silica or hydrocerussite control

In the adsorption experiments with silica on Buffalo scales, all the reactors were started at almost at the same time.

Table 2-9: Sampling time of reactors in one set of experiments with scales

Reaction time	Event
-23.5 h	0.5-hour pre-equilibrium sample
-23 h	1-hour pre-equilibrium sample
-22 h	2-hour pre-equilibrium sample
-20 h	4-hour pre-equilibrium sample
-16 h	8-hour pre-equilibrium sample
0 h	24-hour pre-equilibrium sample
1 min	1-minute sample
5 min	5-minute sample
0.5 h	0.5-hour sample
1 h	1-hour sample
2 h	2-hour sample
4 h	4-hour sample
8 h	8-hour sample
24 h	24-hour sample
48 h	48-hour sample
72 h	72-hour sample
96 h	96-hour sample
96 h	No silica control
96 h	No hydrocerussite control
96 h	No silica or hydrocerussite control

2.2 Analytical Methods

2.2.1 Dissolved Metal Concentrations (Lead and Aluminum)

Samples for dissolved lead and aluminum were analyzed by inductively coupled plasma-mass spectrometry (ICP-MS) (PerkinElmer ELAN DRC II).

Samples of 1mL volume for dissolved lead analysis from each reactor were collected using a 5 mL syringe. Then the samples were filtered through 0.22- μ m polyether sulfone (PES) syringe filters (Tisch Scientific, U.S.A.) and acidified by adding 1 mL of 2% nitric acid and 8 mL of 1% nitric acid according to the requirement of the standard operating procedure for the ICP-MS.

2.2.2 pH

Solution pH was measured with a glass pH electrode and pH meter (Accumet). Standard solutions of pH 4, 7 and 10 were used for calibration prior to each measurement. All samples and standard solutions were stored at room temperature prior to each measurement. Samples were gently stirred, and pH reading were taken soon after the readings of the pH meter stabilized. Ultrapure water was used to rinse the electrode of the pH meter between samples.

2.2.3 Silica Concentration

Samples for dissolved silica concentration measurement (10 mL) from each reactor were collected using a 5 mL syringe. These samples were filtered through 0.22- μ m polyether sulfone (PES) syringe filters (Tisch Scientific, U.S.A.). A colorimetric method, namely the 4500-Si D molybdatesilicate method ^[25], was utilized to measure the silica concentration in a UV-Vis Spectrophotometer at 410 nm. To measure "molybdate-reactive" silica, 0.167M ammonium molybdate reacts with silica and phosphate in 10 mL of sample water to form molybdsilicic acid and molybdophosphoric acid, which gives a yellow color in the solution. The absorbance of the solution can be measured by the spectrometer at a wavelength of 410 nm. Only monomeric silica is detected using this method.

There is a potential interference in the method associated with phosphate. Ammonium molybdate at pH approximately 1.2 reacts with silica and any phosphate present to produce heteropoly acids. This interference is avoided by adding oxalic acid, which destroys the molybdophosphoric acid but not the molybdsilicic acid.

Table 2-10: Reagents used in colorimetric method for measurement of dissolved monomeric silica

Reagent	Concentration	Volume added
Hydrochloric acid	1+1 dilution	0.4 mL
Ammonium molybdate	40 g/L	1 mL
Oxalic acid	30 g/L	1 mL

2.2.4 BET Specific Surface Area Analysis

The specific surface areas of dry solids were determined by the Brunauer-Emmett-Teller-N₂ (BET-N₂) adsorption (Quantachrome Instruments) method. The solid sample was degassed for 13 hours at 100°C before analysis. The analysis temperature was 77.35 K.

2.2.5 X-Ray Diffraction Analysis

XRD patterns were collected using Cu K α radiation (Bruker d8 Advance X-ray diffractometer).

2.2.6 Acid Digestion of Buffalo Scales

Specific amounts (0.1 g) of scales were digested in 20 mL aqua regia (concentrated HNO₃ and HCl in a volumetric ratio of 1:3) in a container at 70°C for an hour. The digested solution was diluted using deionized water (DI water) and to prepare samples for analysis on an inductively coupled plasma mass spectrometer (ICP-MS). Dilution factors of 2500 times and 25000 times were chosen for different metals in the solution to avoid exceeding the detection limit of 200 ppb on ICP-MS.

2.3 Statistical Analysis

Confidence intervals were used for comparison of treatments. All statistical analyses were conducted at the 95% confidence level. All the mathematical models were developed in Matlab and Microsoft Excel using constraints of mass balances and the adsorption reactions.

Chapter 3

Results and Discussion

Experimental results of the two major sets of experiments are presented and discussed in this chapter. The first section of the chapter focuses on adsorption of dissolved silica on hydrocerussite, which is one of the major components of lead pipe scales. The second section will focus on adsorption of dissolved silica on actual scales removed from aged lead pipes that had been in use for decades. These experiments were designed to investigate and compare the behavior of hydrocerussite and scales with respect to uptake of dissolved silica from aqueous solution. Additionally, the effectiveness of pH, initial dissolved silica concentration and mass of solid added are discussed in this chapter.

3.1 Adsorption of Silica on Hydrocerussite (at pH 8.8)

3.1.1 Characterization of Hydrocerussite Used in the Experiments

3.1.1.1 XRD Analysis

The hydrocerussite purchased for use in batch experiments contains hydrocerussite as the dominant crystalline phase on the basis of its XRD pattern (Figure 3-1). However, peaks from plumbonacrite $[\text{Pb}_{10}(\text{CO}_3)_6\text{O}(\text{OH})_6]$ and cerussite $[\text{PbCO}_3]$ are also observed in this pattern.

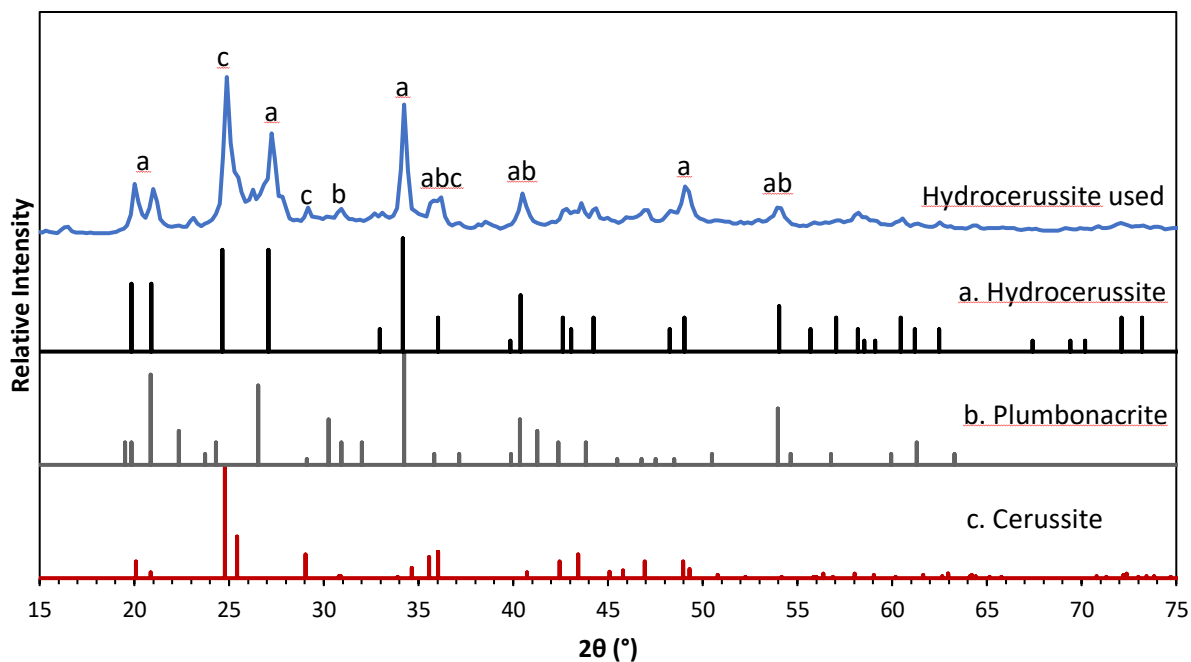


Figure 3-1: Comparison of purchased hydrocerussite and the reference patterns of hydrocerussite and two other solids that appear to be present in this material (the experimental and reference patterns have been scaled so that the intensities of their highest peaks are the same)

3.1.1.2 BET Specific Surface Area Analysis

The specific surface area of the purchased hydrocerussite was measured in a previous project and was determined to be $10.7 \text{ m}^2/\text{g}$.^[26] Additionally, hydrocerussite from different sources used in other studies has been reported to have different specific surface areas. In the research of Kushnir^[27], the surface area of hydrocerussite purchased from Sigma-Aldrich was determined to be $1.16 \pm 0.02 \text{ m}^2/\text{g}$, while Noel et al. found the surface area of hydrocerussite that was synthesized by precipitation from a supersaturated lead carbonate solution to be $4.8 \text{ m}^2/\text{g}$ ^[28].

3.1.2 Change in pH with Time

Once silica and hydrocerussite were added into the reactor, the pH value was adjusted to 8.8 at the beginning of the experiment, and pH values were measured at the same time that samples were collected for measurement of dissolved SiO_2 and Pb. We can see that the pH stayed stable within 8.8-8.9 (Figure 3-2).

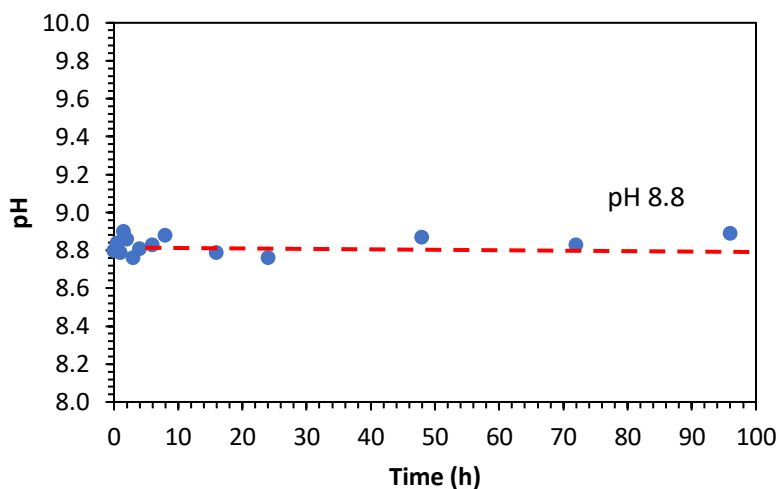


Figure 3-2: pH variation with time (with 0.2 g of hydrocerussite, 20 mg/L silica in 100 mL of solution)

3.1.3 Adsorption Experiments on Hydrocerussite

3.1.3.1 Adsorption Isotherm and Sorption Site Density at pH 8.8

Data from samples collected after a 96-hour equilibration time for different initial silica concentrations (adsorbate) and different amounts of hydrocerussite (adsorbent) were used to prepare a plot (Figure 3-3) from which adsorption isotherms could be evaluated. The C_{eq} is the equilibrium silica concentration ($\mu\text{mol/L}$) obtained at the end of the experiment (96 hours), C_0 is initial silica concentration ($\mu\text{mol/L}$), q is adsorption capacity calculated by eqn. (2) in units of $\mu\text{mol/m}^2$, S is the specific surface area (m^2/g) of hydrocerussite, and V is suspension volume (100 mL in this case).

$$q = \frac{(C_0 - C_f)V/M_{adsorbate}}{m_{adsorbent} \times S_{adsorbent}} \quad (2)$$

The data best fits a linear isotherm (Figure 3-3). As the initial concentration of silica increased, the measured sorption density also increased. In the experiments (Table 2-3: experiments 1-16) carried out with silica concentration within 0 to 50 mg/L as SiO₂, the adsorption capacity of hydrocerussite did not level out at any value as would be observed for a Langmuir isotherm, nor did it have any downward concavity as in a Freundlich isotherm.

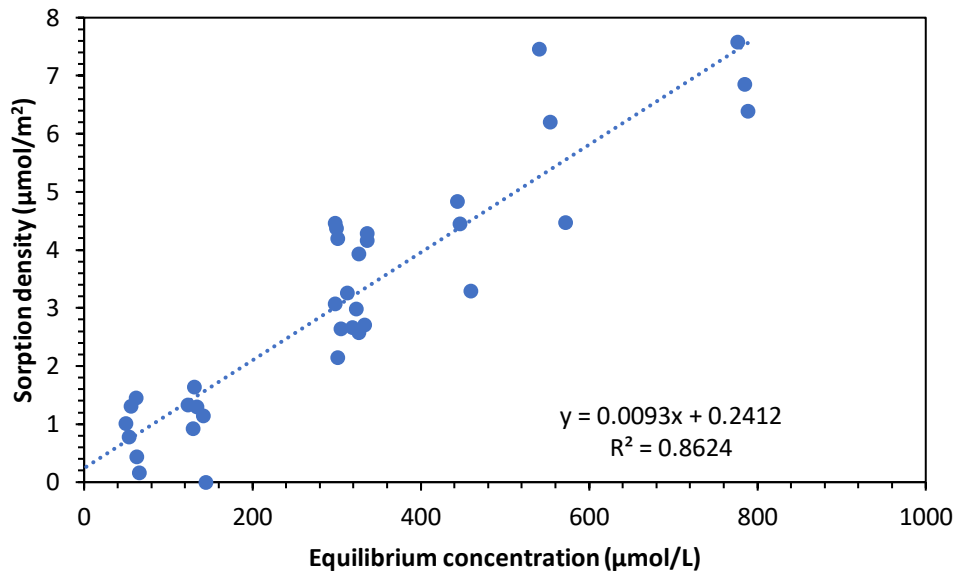


Figure 3-3: Adsorption isotherm of silica on hydrocerussite at pH 8.8 for 96-hour equilibration time

With the adsorbed silica concentrations that we got in the adsorption experiments (Table 2-3: experiments 1-16), we can calculate the surface sites on hydrocerussite that would need to be present if the uptake were occurring due to adsorption of monomeric silica at discrete adsorption sites on the surface. If we take data from experiments 3, 14, 15 and 16 (Figure 3-4) as an example (i.e. those experiments with 0.1 g hydrocerussite in the reactors), we can figure out that for different initial silica concentrations, the average consumption of silica was 3.24 mg/L within 96 hours. Then we can calculate the approximate the surface site density by using eqn. (3):

$$\begin{aligned}
[\text{surface site density}] &= q \times [\text{Avogadro constant}] \\
&= \frac{3.24 \frac{\text{mg}}{\text{L}} \times \frac{1\text{g}}{1000\text{mg}} \times \frac{\text{mol}}{60.08\text{g}} \times \frac{6.02 \times 10^{23} \text{sites}}{\text{mol}}}{0.1\text{g} \times \frac{10.70\text{m}^2}{\text{g}} \times \frac{10^{18}\text{nm}^2}{1\text{m}^2}} \quad (3) \\
&= 30.34 \text{ site/nm}^2
\end{aligned}$$

Based on our experience and relevant research ^{[29][30]}, 30.24 site/nm² is unreasonably high for a mineral surface. Typical site densities of minerals are 1-10 sites/nm². The fact that more dissolved silica uptake occurred than would be possible by monolayer adsorption, means that some additional processes must be responsible for the dissolved silica uptake. Approximately 5-10% of added silica can convert into polymeric silica (~10% hypothesized by Davis et al. in reference [31]). To quantify the effect of formation of polymeric silica, we can assume a 5-10% conversion of monomeric silica. In the end, eliminating 5% of conversion will correspond to a sorption density of 20.98 site/nm² and eliminating 10% of conversion will correspond to a sorption density of 11.61 site/nm², which is closer to but still higher than the upper range of typical surface site densities (10 site/nm²). A more plausible explanation for the high sorption density is the precipitation of amorphous silica whose initial nucleation is facilitated by the surface of hydrocerussite.

3.1.3.2 Silica Uptake Kinetics

The result of the control experiments with silica in the absence of hydrocerussite shows that a small amount of silica (<5%) was lost even if there is no hydrocerussite in the reactors. The dissolved silica that is detected by the analytical technique is only monomeric silica. Consequently, the conversion of some of the dissolved monomeric silica into dissolved polymeric silica could explain this observed decrease in dissolved monomeric silica. It is also possible that silica was adsorbed onto the reactor or stir bar.

Table 3-1: Comparison of equilibrium concentration (with 0.1 g hydrocerussite in 100 mL solution) and final silica concentration in control experiments with no hydrocerussite in experiments 3, 14, 15 and 16 (Table 2-3)

Initial concentration (mg/L)	Equilibrium concentration with hydrocerussite (mg/L)	Final concentration in control experiments (mg/L)	Difference from the initial concentration of control experiment (mg/L)
20.81	18.00	20.24	0.57
29.71	27.01	28.96	0.75
37.25	33.35	36.31	0.94
51.54	47.06	50.58	0.96

The consumption of silica stabilized after 96 hours in the presence of hydrocerussite, which established the equilibrium time used for subsequent experiments. The rate of consumption of silica is faster in the first 4 hours than in the following 92 hours. The percentage of consumed silica is always below 15% in all the experiments. The extent of the decrease in the silica concentration when in contact with 0.1 g hydrocerussite was similar for different initial silica concentration and was within 3-4 mg/L SiO₂, while the amount of silica consumed increased with increasing amount of hydrocerussite.

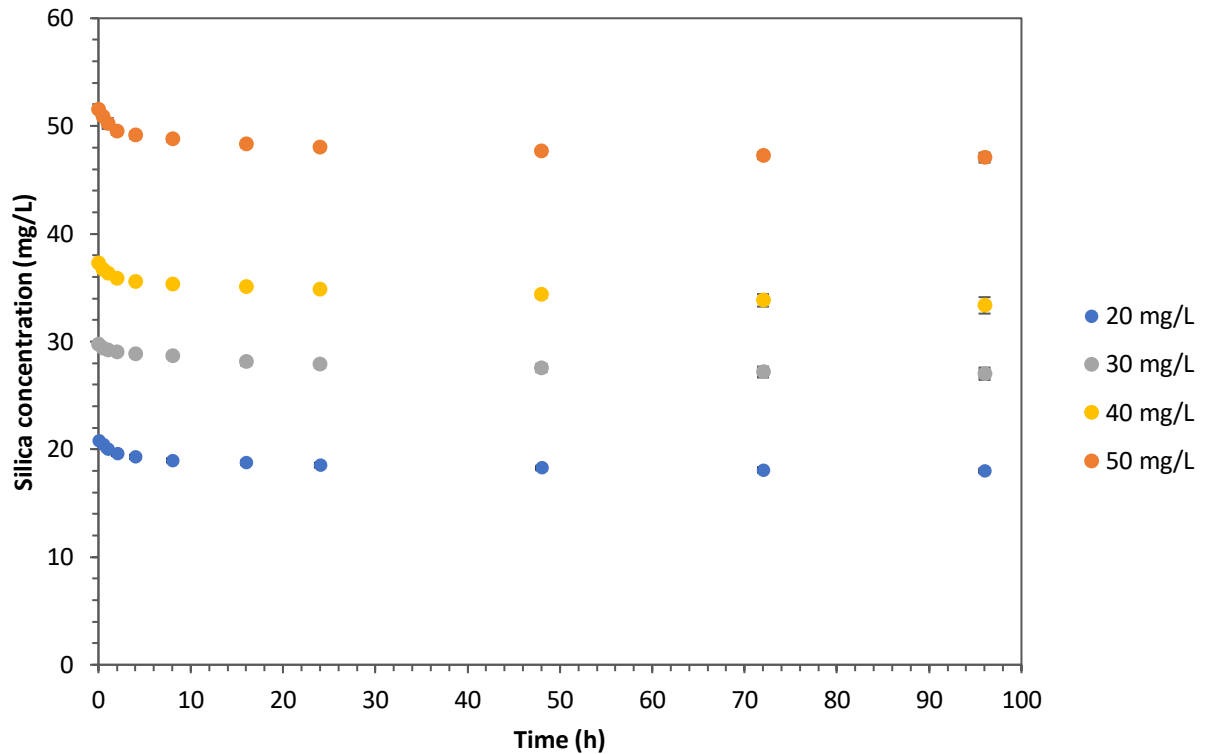


Figure 3-4: Variation in dissolved silica concentration with time for different initial silica concentrations with 0.1 g hydrocerussite in the reactor (in 100 mL of water, which makes the concentration of hydrocerussite 1 g/L) in experiments 3, 14, 15 and 16 (Table 2-3). Error bars are showing 1 standard deviation. The initial concentrations of silica in the series labeled 20, 40 and 50 mg/L case were not exactly 20, 40 and 50 because of an experimental error (<5%) in the addition of solutions to prepare the reactors.

Table 3-2: Average removal of dissolved silica in experiments 1-6 (Table 2-3) with 20 mg/L silica was added

Hydrocerussite added (g/L)	Average removal (mg/L)
0.25	0.63
0.50	1.01
0.75	1.30
1.00	1.85
1.50	2.70
2.00	2.64

Considering the uptake rate of silica shown in the silica concentration plots (Figure 3-4) and the mechanism of adsorption reactions, we hypothesize that the uptake rate of silica

follows a *pseudo*-first-order differential equation with respect to silica concentration (eqn. (4)):

$$\frac{dC}{dt} = -k[\text{hydrocerussite}]^n(C - C_{eq}) \quad (4)$$

Where C_{eq} represents the 96-hour silica concentration, which is considered as the equilibration point.

Equation (4) can be integrated:

$$C - C_{eq} = (C_0 - C_{eq})e^{-k[\text{hydrocerussite}]^n t} \quad (5)$$

Taking the natural log on both sides yields:

$$\ln \frac{C_0 - C_{eq}}{C - C_{eq}} = k[\text{hydrocerussite}]^n t \quad (6)$$

If we let $k' = k[\text{hydrocerussite}]^n$, where k' is the pseudo-first-order rate constant of silica uptake with respect to silica concentration, then we can obtain a linear model (eqn. (7))

$$\ln \frac{C_0 - C_{eq}}{C - C_{eq}} = k' t \quad (7)$$

Table 3-3: Constants used in modeling the uptake rate of silica by hydrocerussite (the model is using g/L as the units for the amount of hydrocerussite, but the uptake is actually controlled by the surface area which is linearly proportional to the mass)

Constants	Definitions	Units	Value of constants
C_0	Initial silica concentration	$mmol \cdot L^{-1}$	-
C_{eq}	Equilibrium silica concentration	$mmol \cdot L^{-1}$	-
k	Rate constant of silica taken up by hydrocerussite	$L^n \cdot g^{-n} \cdot h^{-1}$	0.0449
k'	<i>Pseudo</i> -first-order rate constant of silica taken up by hydrocerussite	h^{-1}	-
[hydrocerussite]	Mass of hydrocerussite	$g \cdot L^{-1}$	0.25-2.00
n	Reaction order of hydrocerussite	-	0.0303

On comparison of experimental data with the model output, we can observe that the model does not fit the data well in the first 4 hours. The uptake at the beginning of the reaction is faster than that predicted by the model. The model has a better fit at longer times of reaction.

Also, from the constants obtained from the model we can see that the reaction order of hydrocerussite with respect to silica concentration is a quite small number (0.0303), which indicates that the reaction rate is insensitive to the amount of hydrocerussite added.

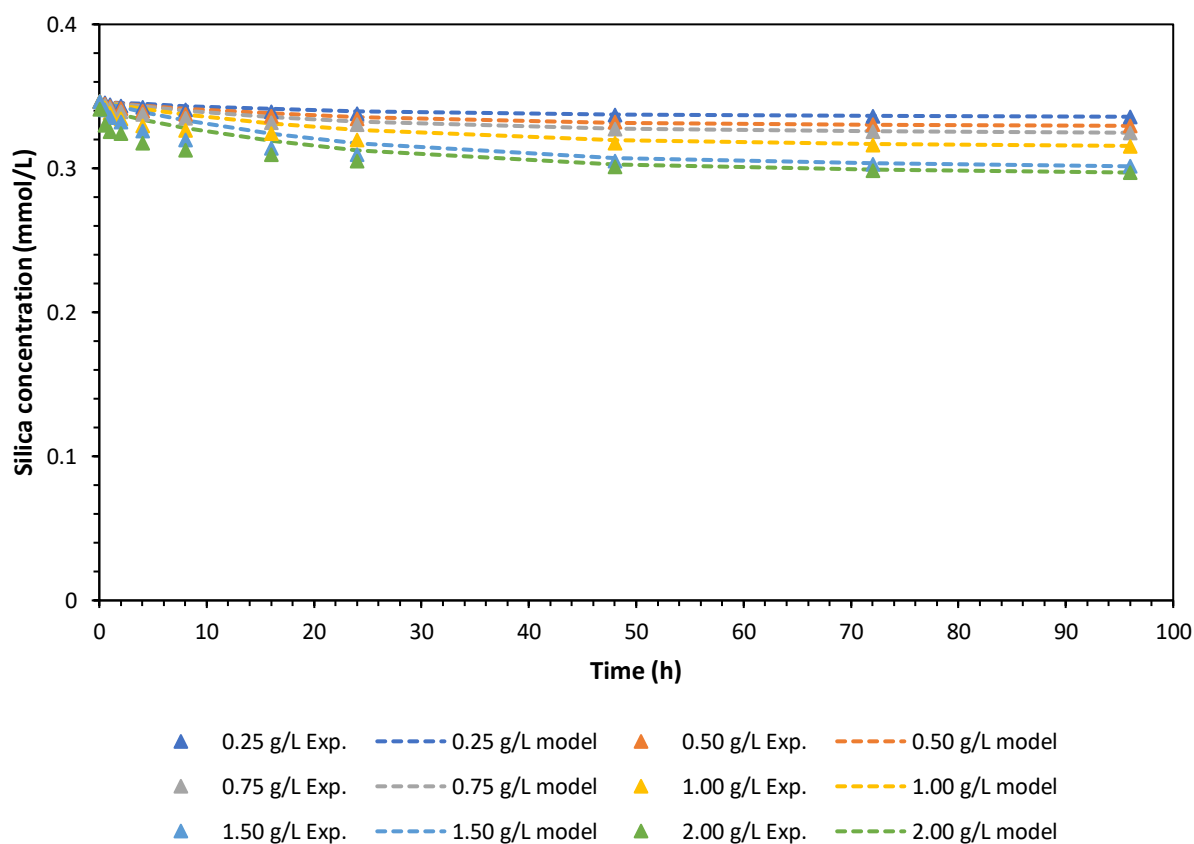


Figure 3-5: Experimental data (experiments 1-6 in Table 2-3) compared with model output (initial silica concentration is 0.35 mmol/L= 20 mg/L)

If we plot the model and compare it with experimental data, then we can see that the model is not the best fit. In the first a few hours, there is a rapid uptake and after that the reaction rate decreases before equilibrium is approached. Based on this difference between the monophasic model and experimental data, we decided to interpret the rate of silica uptake

of silica using a biphasic model. Also, since the initial model of monophasic kinetics indicated that the rate of uptake was not very sensitive to the amount of hydrocerussite present, the biphasic model was developed by considering the process of consistent of two pseudo first-order processes. This results in the optimization of a model with only two fitting parameters (k_1 and k_2) to the experimental data of silica uptake:

$$C - C_{eq} = (C_0 - C_{eq})(e^{-k_1t} + e^{-k_2t}) \quad (8)$$

Constant k_1 is related to the rate of the of the faster process, and k_2 determines the rate of the slower process. Therefore, the first exponential term will dominate the reaction rate in the fast stage and the second term will dominate the reaction rate in the slow stage. Values of the constants obtained are shown below:

Table 3-4: Constants used in the biphasic modeling equation

Constants	Definitions	Units	Value of constants
C_0	Initial silica concentration	$mmol \cdot L^{-1}$	-
C_{eq}	Equilibrium silica concentration	$mmol \cdot L^{-1}$	-
k_1	Rate constant of silica taken up by hydrocerussite in term 1	h^{-1}	0.6499
k_2	Rate constant of silica taken up by hydrocerussite in term 2	h^{-1}	0.0405

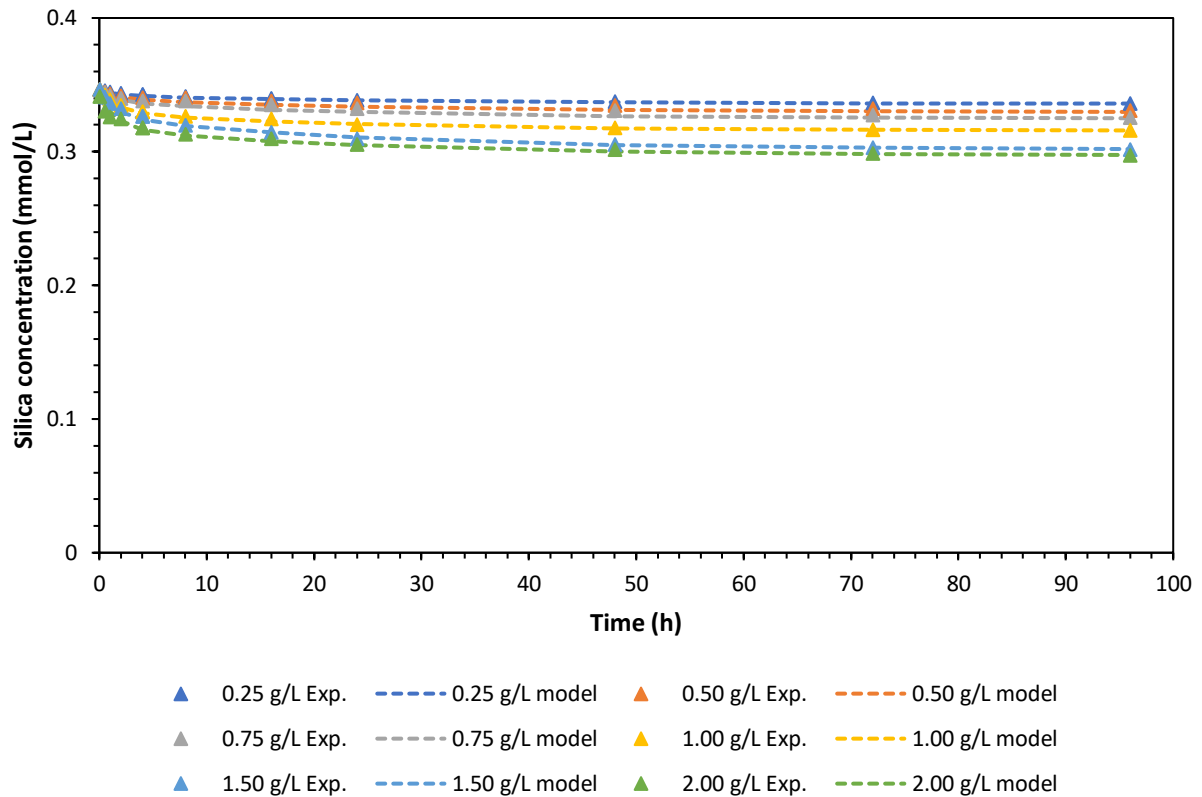


Figure 3-6: Experimental data (experiments 1-6 in Table 2-3) compared with biphasic model at pH 8.8 (initial silica concentration is 0.35 mmol/L=20 mg/L)

Comparing the plot of the biphasic model and experimental data, we can see that the model provides a better fit to the data than does the monophasic model, which indicates that the uptake of silica by hydrocerussite is possibly controlled by two separate processes. The model also works well over a range of hydrocerussite concentrations, which confirms that the rate constants for the uptake are independent of the amount of hydrocerussite present. As discussed earlier, the final equilibrium concentration is affected by the amount of hydrocerussite. The biphasic model also provided good fits to the experimental data for different initial dissolved silica concentrations and 1 g/L hydrocerussite at pH 8.8 (Figure 3-7).

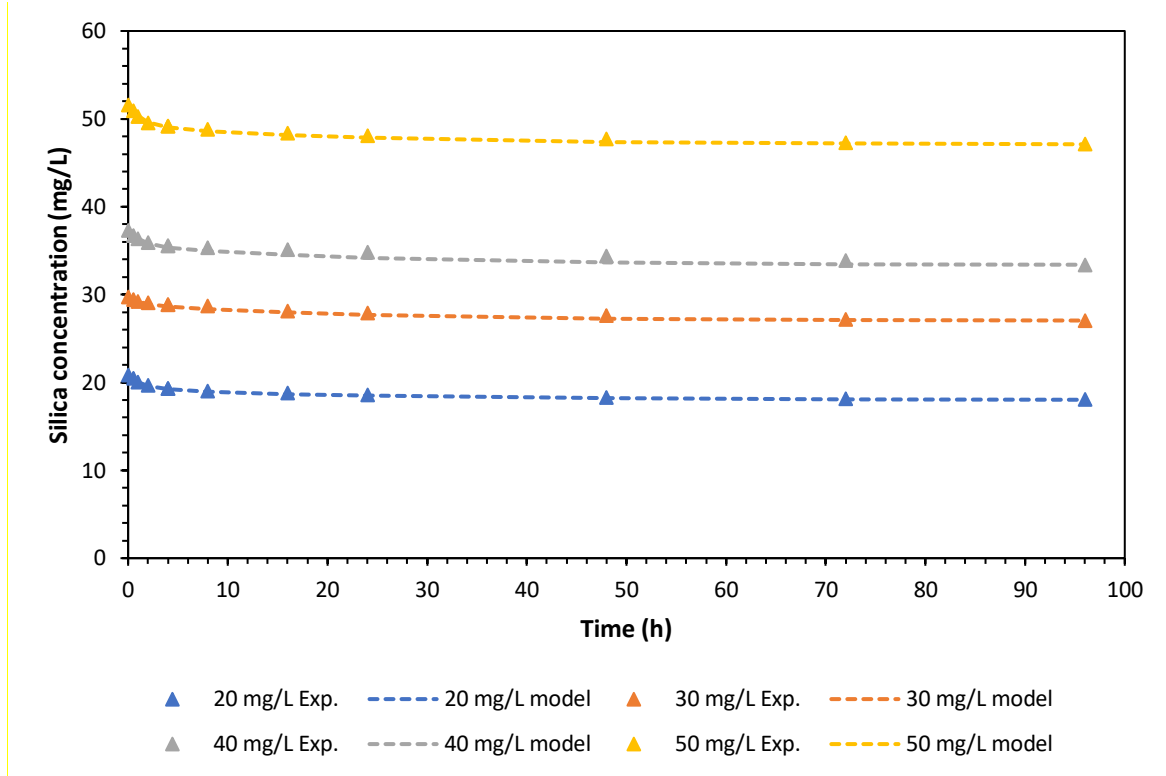


Figure 3-7: Experimental data (experiments 3, 14, 15, 16 in Table 2-3) compared with biphasic model at pH 8.8 (concentration of hydrocerussite in the reactors is 1 g/L)

3.1.4 Change of Lead Concentration with Time

The dissolved lead concentration fluctuated around 110 $\mu\text{g/L}$ with time. There was not much difference between the lead concentration in the experimental group and in the control group that had only hydrocerussite and no added dissolved silica, which indicates that silica addition did not inhibit the dissolution of hydrocerussite.

Based on the equilibrium solubility of hydrocerussite (Figure 1-2) at Buffalo water conditions with DIC at 24 mg/L as C, alkalinity of 93 mg/L as CaCO_3 and the ionic strength about 0.0026 M, the theoretical lead concentrations at pH 8.8 is 45 $\mu\text{g/L}$ according to the calculation in *MINEQL+*, which is much lower than 110 $\mu\text{g/L}$. The equilibrium solubility is calculated with the solubility constants, dissociation constants and stability constants taken assuming the reactions occurred at standard conditions at 25°C, while the

use of real values for these constants can result in different lead concentrations. Also, the presence of other unidentified phases in the XRD pattern of hydrocerussite used in these experiments, however in low amounts, could yield a higher dissolved lead concentration that is predicted for pure hydrocerussite.

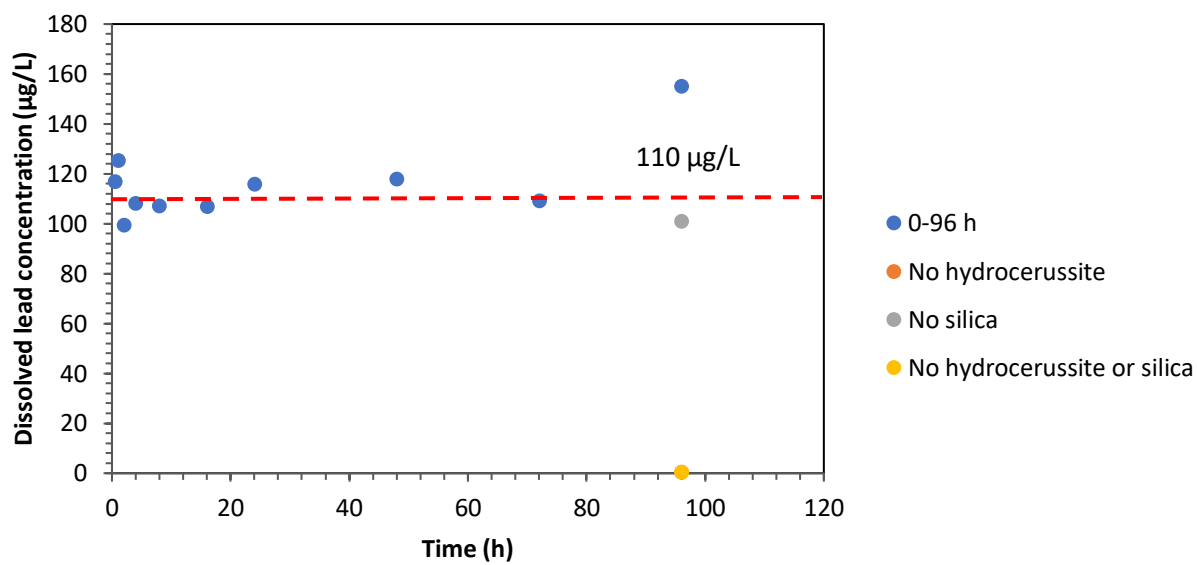


Figure 3-8: Variation in dissolved lead concentration with time (with 0.2 g of hydrocerussite and 20 mg/L silica in 100 mL of water at pH 8.8) the yellow point and orange point are overlapping with each other

3.2 Adsorption of Silica on Scales Removed from Lead Service Lines from Buffalo

3.2.1 Characterization of Scales Used in the Experiments

3.2.1.1 XRD Analysis

According to the XRD analysis, hydrocerussite is detected as the dominant phase of lead in the scales and small quantities of plattnerite (β - PbO_2) and elemental lead are also present in the scale. Crystalline silica or quartz is also present in the scale, but this may be present from parts of the soil that may have gotten into the pipe during installation or during harvesting of the pipe. Broad peaks between 8 to 15 degrees indicate that an amorphous or

poorly crystalline mineral is present in the scale; we are unable to identify it without further characterization. There is a minor phase containing aluminum minerals which should also be in the scales based on the acid digestion of scales.

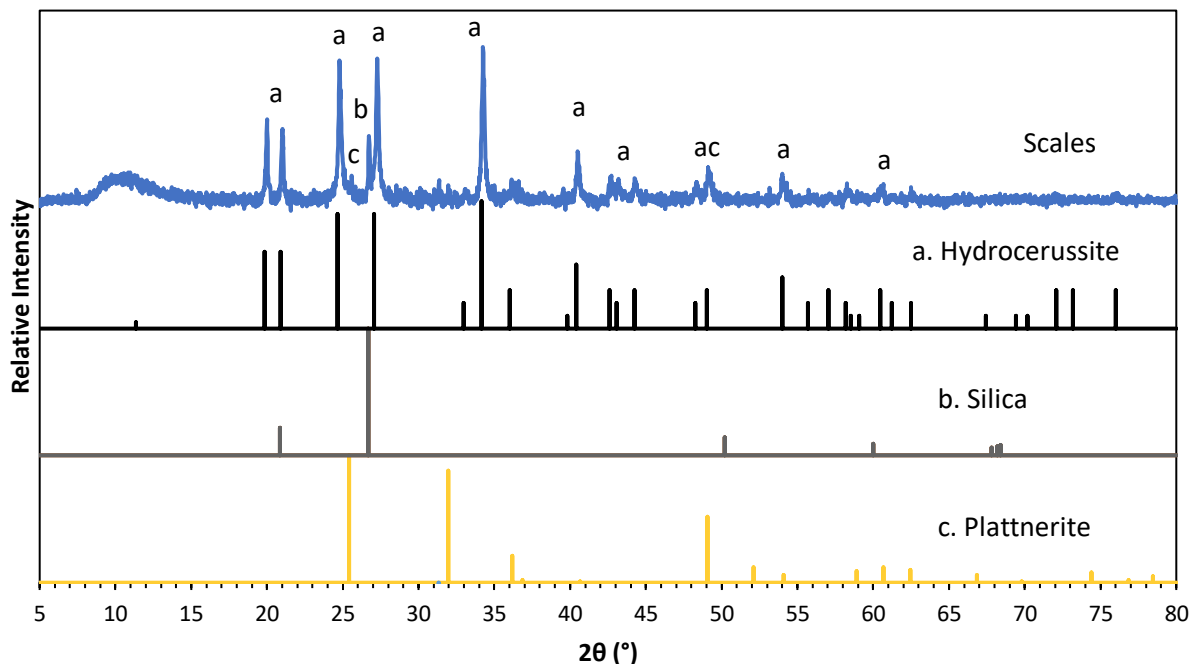


Figure 3-9: XRD comparison of procured Buffalo scales and the standard pattern of hydrocerussite (the experimental and reference patterns have been scaled so that the intensities of their highest peaks are the same)

3.2.1.2 Acid Digestion of Scales

According to the result of ICP-MS, the concentrations of Pb and Al in the 25000-times diluted sample from the digestion of 0.100 g of scale were 53.7 $\mu\text{g/L}$ and 40.0 $\mu\text{g/L}$, respectively. Thus, we can calculate their mass fractions in the scales:

$$Pb\% = 53.7 \frac{\mu\text{g}}{\text{L}} \times 25000 \times 20 \text{ ml} \times \frac{1 \text{ L}}{1000 \text{ ml}} \times \frac{1 \text{ g}}{1000000 \mu\text{g}} \times \frac{1}{0.1 \text{ g}} = 26.9\% \quad (9)$$

$$Al\% = 40.0 \frac{\mu\text{g}}{\text{L}} \times 25000 \times 20 \text{ ml} \times \frac{1 \text{ L}}{1000 \text{ ml}} \times \frac{1 \text{ g}}{1000000 \mu\text{g}} \times \frac{1}{0.1 \text{ g}} = 20.0\% \quad (10)$$

3.2.1.3 BET Specific Surface Area Analysis

The BET analysis determined a surface area of 150 m²/g, which is much higher than the specific surface area of 10.7 m²/g for the hydrocerussite studied in the experiments discussed in Section 3.1. The high surface area could be contributed by other mineral phases such as unidentified aluminum-rich amorphous solids.

3.2.2 Change in pH with Time

The scales when exposed to Buffalo water with sodium silicate at 20 mg/L as SiO₂ was measured to be at pH of 8.8 and 7.7. From Figure 3-10 and Figure 3-11 we can see that after the addition of scales and pH adjustment in the reactor, the pH in both reactors did not change much with time.

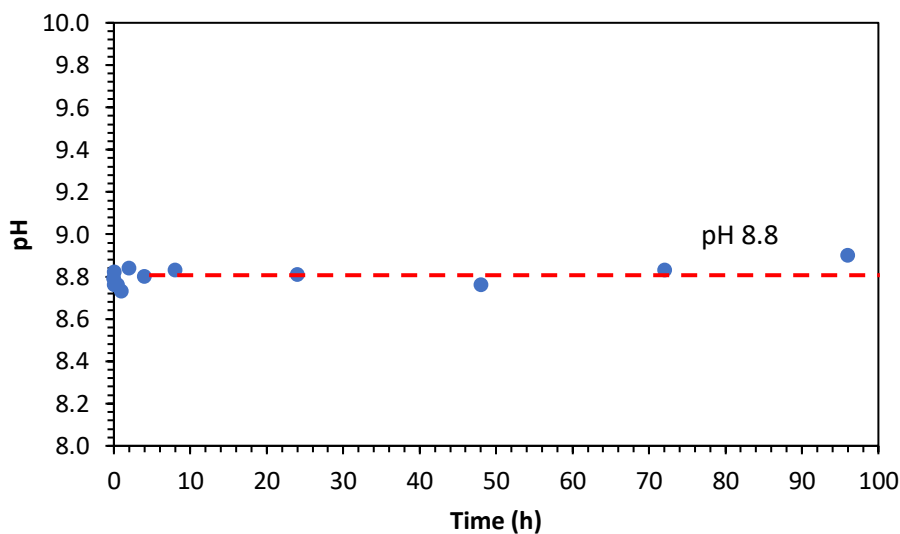


Figure 3-10: pH variation with time with an initial pH of 8.8 (with 0.1 g of scales and 20 mg/L silica in 50 mL of solution)

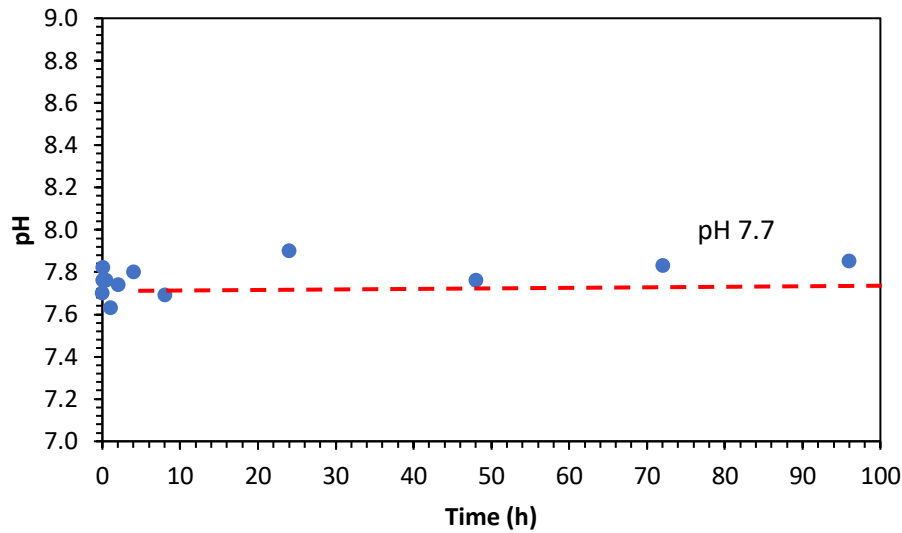


Figure 3-11: pH variation with time with an initial pH of 7.7 (with 0.1 g of scales and 20 mg/L silica in 50 mL of solution)

3.2.3 Mechanism of silica uptake

Silica uptake by Buffalo scales was much higher than that by pure hydrocerussite. Scales consumed 65% of silica which was four-fold higher than the 15% consumption by the same concentration of pure hydrocerussite. The high consumption of silica can be attributed to the high surface area of the scale allowing more surface interaction. We can also infer that minerals other than hydrocerussite are reacting with silica.

Silica concentration dropped from 20 mg/L to around 7 mg/L with time. A rapid uptake of silica took place in the first few minutes, which has been reported previously [24]. According to the first few experiments, the equilibrium time of silica uptake is around 96 hours, which can be indicated by figures below. In the comparison of experimental data with different initial silica concentrations (Figure 3-12), we can see silica concentration decreased from 20 mg/L to 7 mg/L (65% consumption) and from 9 mg/L to 2.5 mg/L (72% consumption). Unlike the experiments with hydrocerussite where loss in silica concentration was constant around 3 to 4 mg/L irrespective of the initial concentration, the loss in dissolved silica is nearly constant for the initial dissolved silica concentrations reacting with pipe scale. This

suggests a potentially different mechanism of silica uptake by the scales than by the hydrocerussite. It is likely that upon dissolution of sodium silicate in water, only a certain percentage of silica is available for uptake by the scales. At pH 8.8, almost 70 % of the monomeric species available is in the form of orthosilicic acid and the remaining is the conjugate base. Therefore, it can be inferred that the orthosilicic acid $[\text{Si}(\text{OH})_4]$ is mainly interacting with the scales.

However, based on this logic the loss in silica at pH 7.7 should have been higher than 8.8 since the dissolved silica at pH 7.7 is almost entirely orthosilicic acid. But we need to keep in mind that the interaction of orthosilicic acid takes place with other elements in the scale. Since there is less similarity in the phenomenon of uptake due to hydrocerussite, the other major element that could be responsible is aluminum in the scale. At pH 7.7, the concentration of dissolved aluminum is lower than that seen at high pH. Therefore, uptake of orthosilicic acid may be limited by the concentration of dissolved aluminum while at pH 8.8, the uptake is limited by the concentration of silica.

Aluminum has been observed in the scales of pipes in distribution system. Aluminum comes from the treatment process where the alum or PACl is used for coagulation. The presence of aluminum is also known as a sink for silica in water and can be a major factor in controlling the silica uptake.

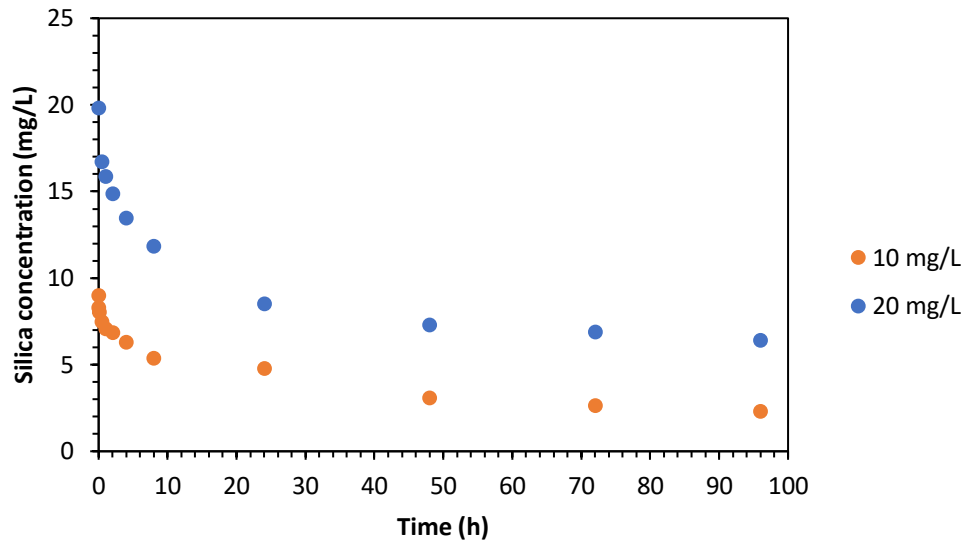


Figure 3-12: Silica concentration variation with time for different silica initial concentrations in experiments 5 and 6 (Table 2-7) (with 0.1 g of scales in 50 mL of solution at pH 8.8), duplicates are performed for this experiment.

Table 3-5: Average removal of dissolved silica for different initial silica concentrations at pH 8.8 and difference of final silica concentration in control experiments with no scales from initial silica concentration in experiments 5 and 6 (Table 2-7)

Silica added (mg/L)	Average silica removal (mg/L)	Difference of silica control from initial conc. (mg/L)
19.82	13.44	0.69
8.98	8.06	0.35

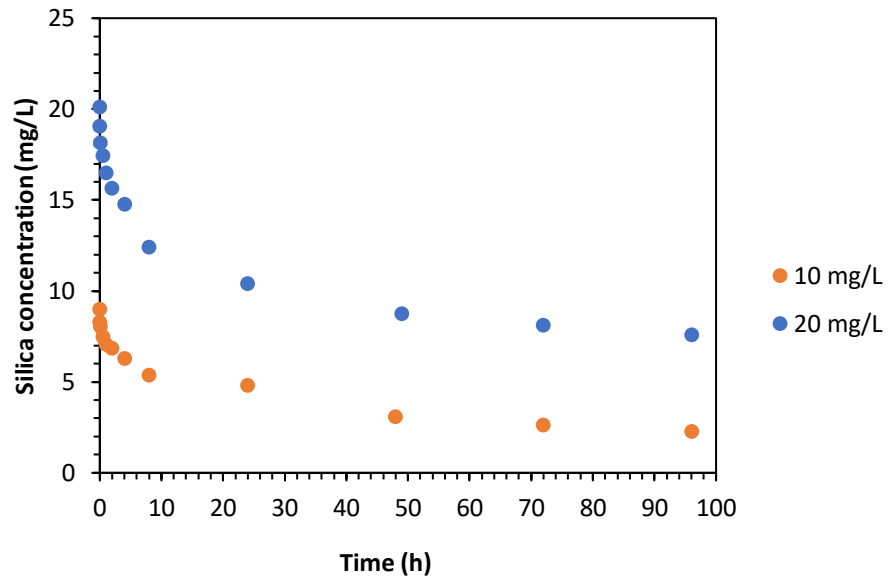


Figure 3-13: Silica concentration variation with time for different silica initial concentrations in experiments 1 and 4 (Table 2-7) (with 0.1 g of scales in 50 mL of solution at pH 7.7), duplicates are performed for this experiment.

Table 3-6: Average removal of dissolved silica for different initial silica concentrations at pH 7.7 and difference of final silica concentration in control experiments with no scales from initial silica concentration in experiments 1 and 4 (Table 2-7)

Silica added (mg/L)	Average silica removal (mg/L)	Difference of silica control from initial conc. (mg/L)
20.12	12.53	0.57
9.56	6.71	0.27

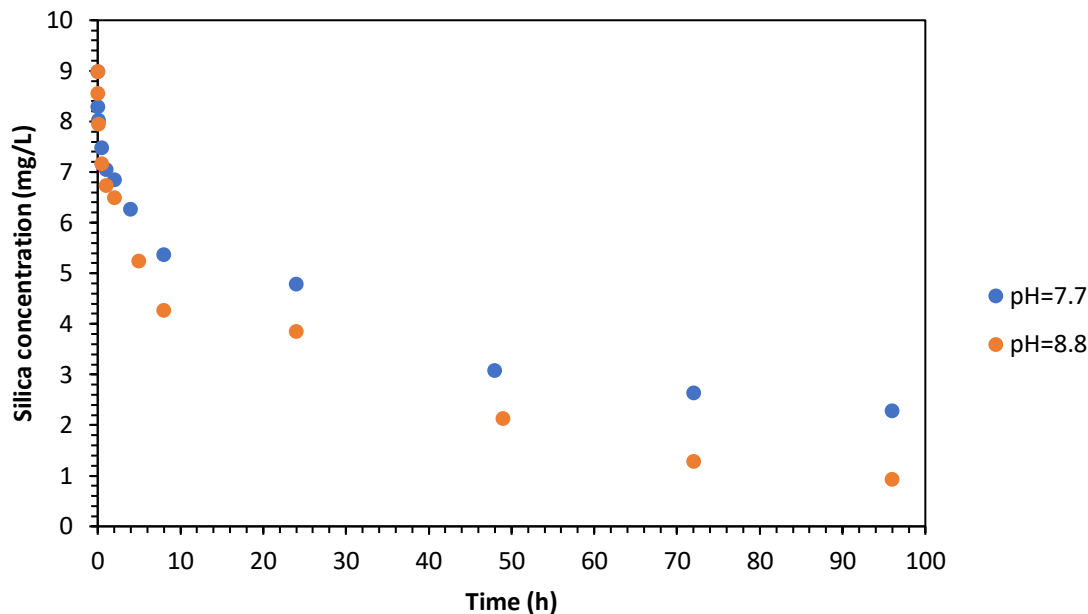


Figure 3-14: Silica concentration variation with time for different pH values in experiments 4 and 5 (Table 2-7) (initial silica concentration = 9 mg/L, scale amount = 0.1 g), duplicates are performed for this experiment.

Table 3-7: Average removal of dissolved silica at pH 7.7 and 8.8 and difference of final silica concentration in control experiments with no scales from initial silica concentration in experiments 4 and 5 (Table 2-7) (initial silica concentration = 9 mg/L, scale amount = 0.1 g)

pH	Average silica removal (mg/L)	Difference of silica control from initial conc. (mg/L)
7.7	6.71	0.27
8.8	8.06	0.35

When the sorption data of silica on Buffalo scales are plotted as an adsorption isotherm (Figure 3-15a), we can see that the sorption density of the scales is much higher than that of hydrocerussite with a unit of $\mu\text{mol/g}$. However, if we plot the isotherm again with $\mu\text{mol/m}^2$ as the unit of sorption density (Figure 3-15b), the sorption density will not be very different from that of hydrocerussite. This observation indicates that the uptake of dissolved silica is controlled by the surface area present in the reactors and it is possible that the uptake does not depend on which solid is contributing to the surface area.

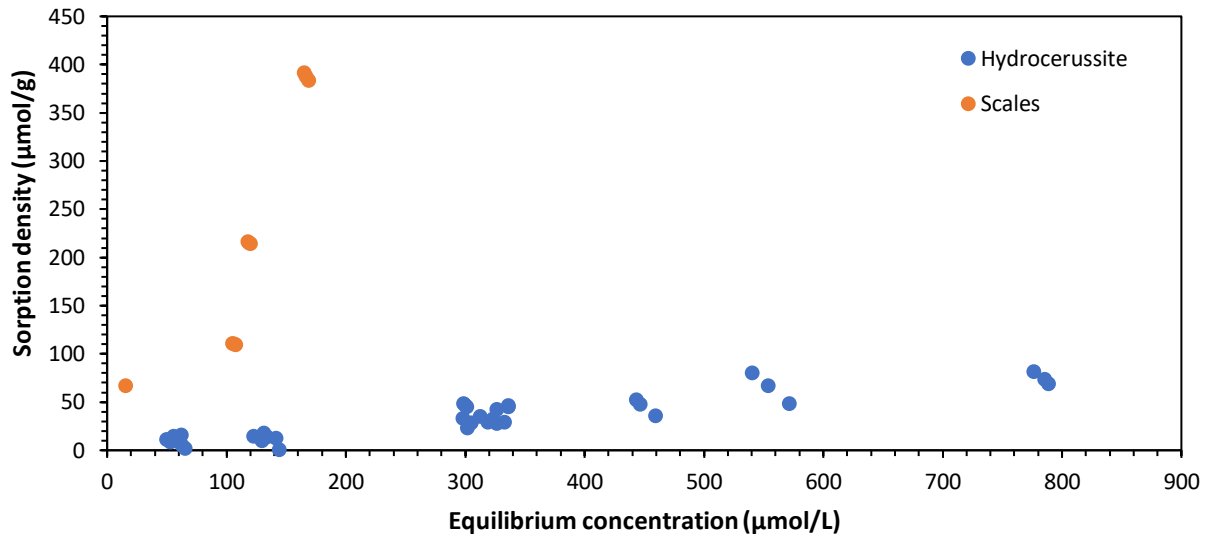


Figure 3-15a: Comparison of adsorption isotherm of silica on hydrocerussite and scales at pH 8.8 for 96-hour equilibration time (unit of sorption density µmol/g)

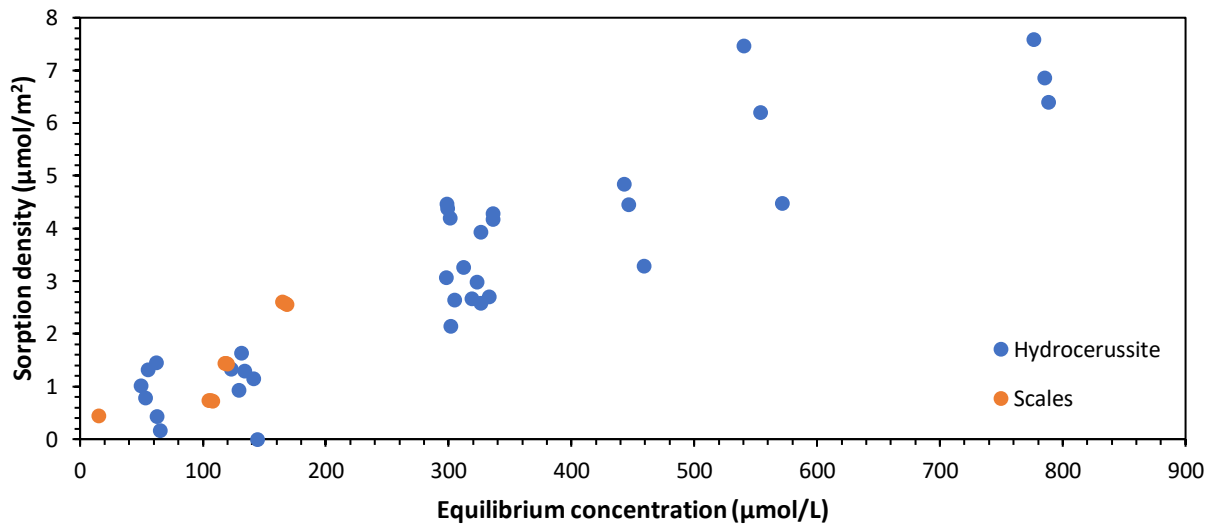


Figure 3-15b: Comparison of adsorption isotherm of silica on hydrocerussite and scales at pH 8.8 for 96-hour equilibration time (unit of sorption density µmol/m²)

Based on the experimental data we can see an increased loss in silica with increasing amounts of scales. The percentage of uptake is shown in Table 3-7. This is similar to the increasing loss in silica seen with increasing amounts of hydrocerussite.

From Figure 3-16 and Figure 3-17 we can see that the uptake of silica is decreasing as the amount of scales is decreasing, which indicates the capacity of scales is limited.

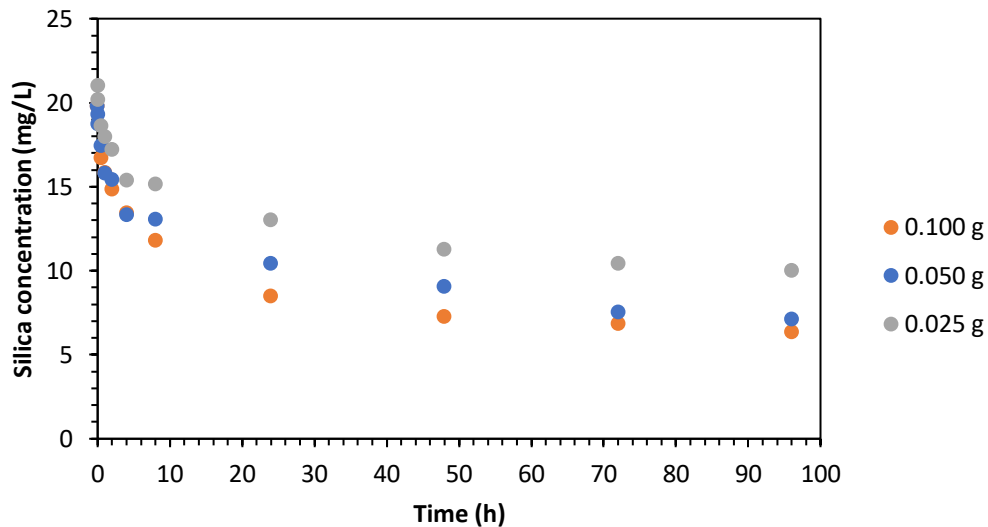


Figure 3-16: Silica concentration variation with time for different amounts of scales in experiments 2, 3 and 6 (Table 2-7) (initial silica concentration = 20 mg/L, pH = 8.8), duplicates are performed for this experiment.

Table 3-7: Silica removal by different amounts of silica at pH 8.8 in experiments 2, 3 and 6 (Table 2-7) with initial silica concentration = 20 mg/L

Scales added (g/L)	0.50	1.00	2.00
Average removal (mg/L)	11.86	12.68	13.44
Average removal (%)	52.38	63.98	67.81

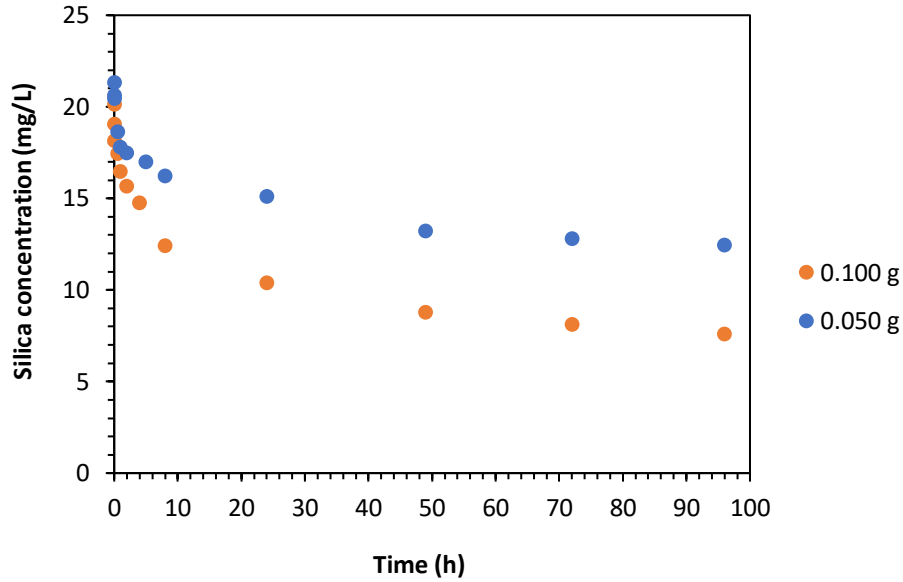


Figure 3-17: Silica concentration variation with time for different amounts of scales in experiments 1 and 7 (Table 2-7) (initial silica concentration = 20 mg/L, pH = 7.7), duplicates are performed for this experiment.

Table 3-8: Silica removal by different amounts of silica at pH 7.7 in experiments 1 and 7 (Table 2-7) with initial silica concentration = 20 mg/L

Scales added (g/L)	1.00	2.00
Average removal (mg/L)	8.88	12.53
Average removal (%)	42	62

A similar kinetic model is explored for the uptake of silica in scales. We assume that the uptake rate of silica follows eqn. (11):

$$\frac{dC}{dt} = -k[\text{scale}]^n(C - C_{eq}) \quad (11)$$

Equation (11) can be integrated:

$$C - C_{eq} = (C_0 - C_{eq})e^{-k[\text{scale}]^n t} \quad (12)$$

Take natural log of both sides:

$$\ln \frac{C_0 - C_{eq}}{C - C_{eq}} = k[\text{scale}]^n t \quad (13)$$

If we let $k' = k[\text{scale}]^n$,

We can obtain a linear model which starts from the origin:

$$\ln \frac{C_0 - C_{eq}}{C - C_{eq}} = k't \quad (14)$$

Table 3-9: Constants used in the modeling equation (the model is using g/L as the unit of amount of hydrocerussite, but the uptake is actually controlled by the surface area which is linearly proportional to the mass)

Constants	Definitions	Units	Value of constants		
C_0	Initial silica concentration	$mmol \cdot L^{-1}$	-		
C_{eq}	Equilibrium silica concentration	$mmol \cdot L^{-1}$	-		
k	Rate constant of silica taken up by scales	$L^n \cdot g^{-n} \cdot h^{-1}$	0.0414 (pH 7.7) 0.0429 (pH 8.8)		
k'	Pseudo-first order rate constant of silica taken up by scales	h^{-1}	0.0417 (pH 8.8)	0.0414 (pH 7.7) 0.0420 (pH 8.8)	0.0423 (pH 7.7) 0.0450 (pH 8.8)
[scale]	Mass of scales	$g \cdot L^{-1}$	0.25	0.50	1.00
n	Reaction order of scales	-	0.0330 (pH 7.7) 0.0542 (pH 8.8)		

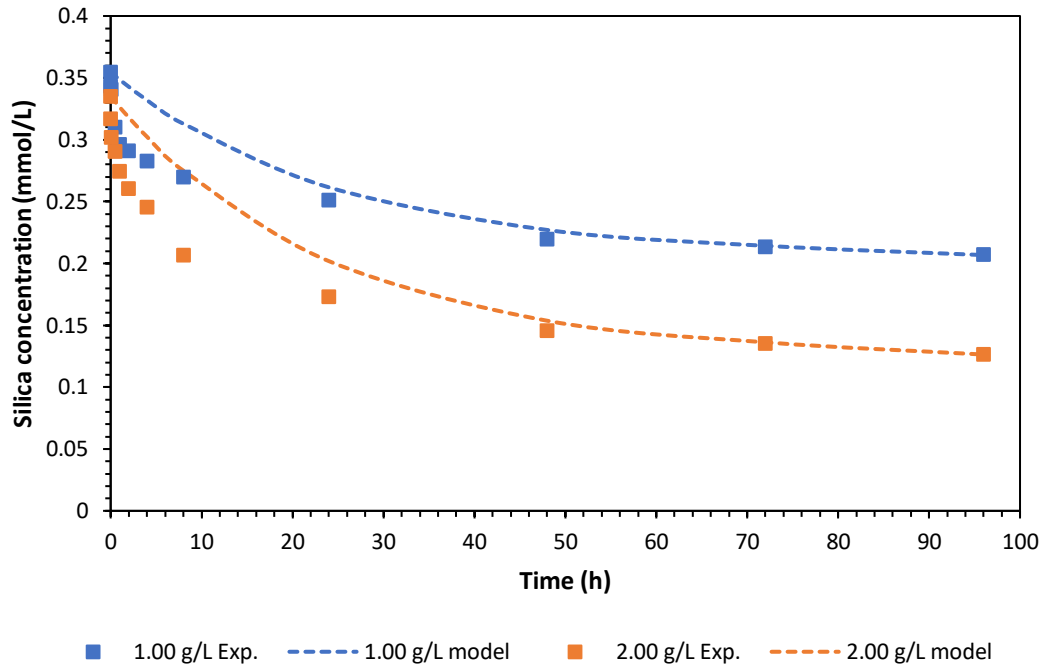


Figure 3-18: Experimental data compared with built model at pH 7.7 in experiments 1 and 7 (Table 2-7) (initial silica concentration is 0.35 mmol/L=20 mg/L)

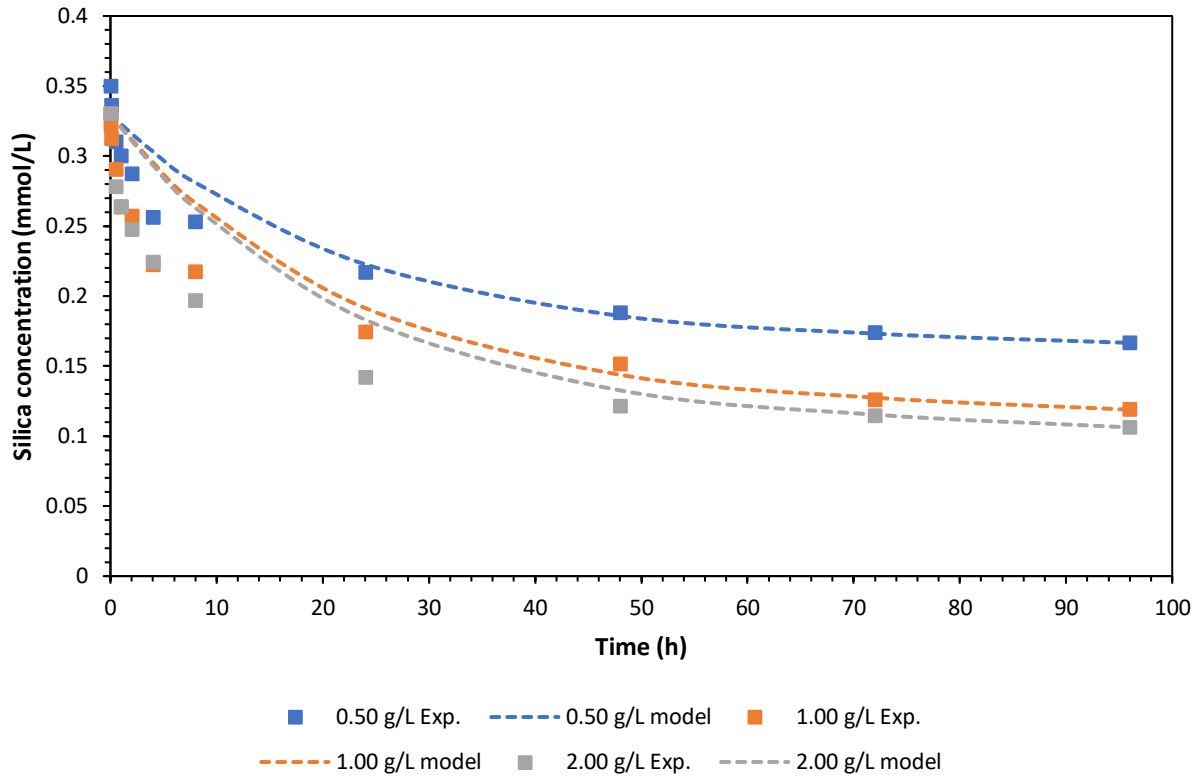


Figure 3-19: Experimental data compared with built model at pH 8.8 in experiments 2, 3 and 6 (Table 2-7) (initial silica concentration is 0.35 mmol/L=20 mg/L)

If we plot the model and compare it with experimental data, we can see that the model is not the best fit. In the first few hours, there is a rapid uptake and after that the reaction rate drastically slows down before equilibrium point. In this circumstance, the reaction rate is still not sensitive to the added mass of scales as we can see from the reaction order of scales with respect to silica concentration (0.0330 and 0.0542). Based on this difference between the monophasic model and experimental data, we decided to interpret the rate of uptake of silica as a biphasic process with two pseudo first-order processes:

$$C - C_{eq} = (C_0 - C_{eq})(e^{-k_1 t} + e^{-k_2 t}) \quad (15)$$

The first exponential term will dominate the rate of uptake in the fast stage and the second term will dominate the rate of uptake for the slow stage. Values of the constants obtained are shown below:

Table 3-10: Constants used in the biphasic modeling equation

Constants	Definitions	Units	Value of constants	
			pH 7.7	pH 8.8
C_0	Initial silica concentration	$mmol \cdot L^{-1}$	-	
C_{eq}	Equilibrium silica concentration	$mmol \cdot L^{-1}$	-	
k_1	Rate constant of silica taken up by scales in term 1	h^{-1}	1.0872	0.6220
k_2	Rate constant of silica taken up by scales in term 2	h^{-1}	0.0377	0.0383

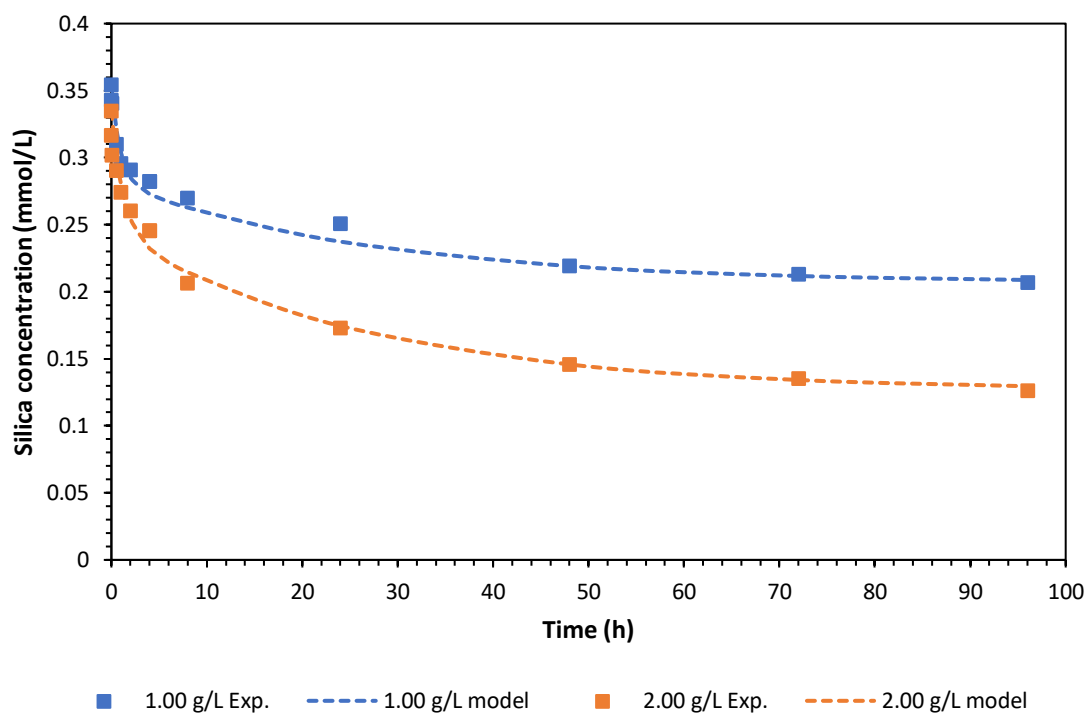


Figure 3-20: Experimental data compared with biphasic model at pH 7.7 in experiments 1 and 7 (Table 2-7) (initial silica concentration is 0.35 mmol/L=20 mg/L)

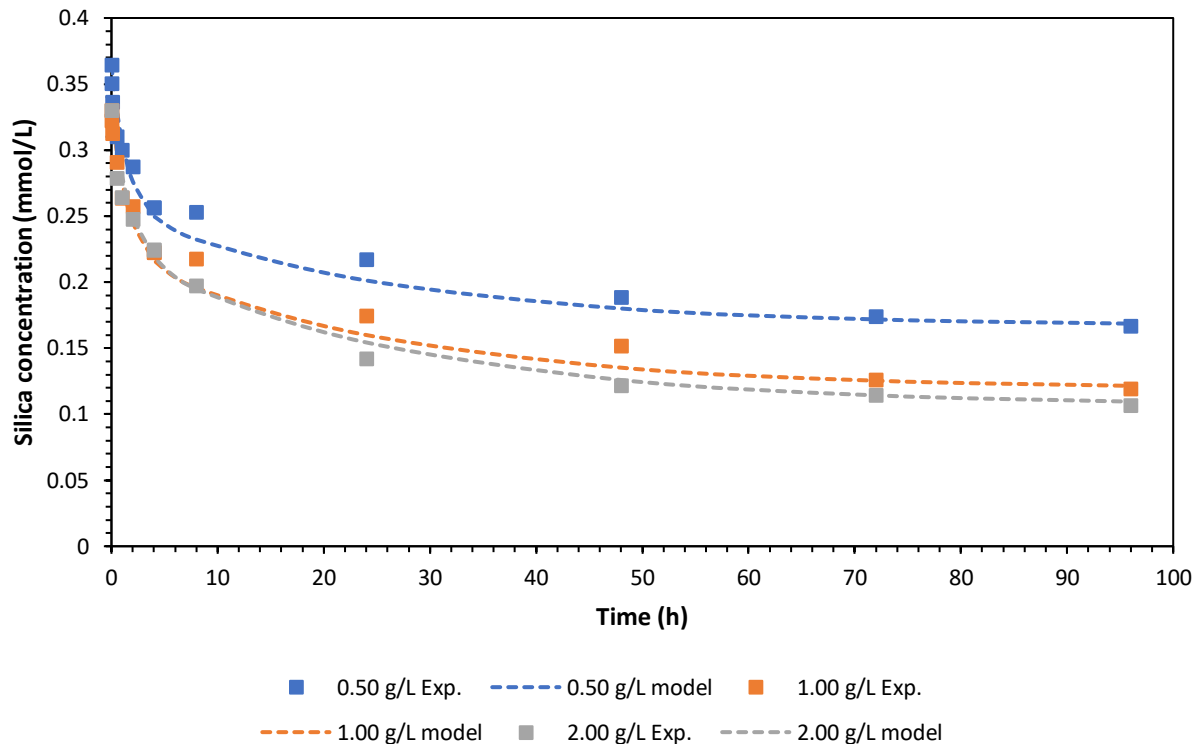


Figure 3-21: Experimental data compared with biphasic model at pH 8.8 in experiments 2, 3 and 6 (Table 2-7) (initial silica concentration is 0.35 mmol/L=20 mg/L)

Comparing the plot of the biphasic model and experimental data, we can see that the model is a better fit than the monophasic model, which indicates that the uptake of silica by the scales are possibly controlled by two subsequent interactions.

3.2.4 Change of Lead and Aluminum Concentration with Time

At pH 7.7, after the addition of silica and pH adjustment in the reactor, the lead concentration began to fluctuate in the range of 100-150 $\mu\text{g/L}$ with time. These concentrations were higher than 75 $\mu\text{g/L}$ seen during the pre-equilibrium experiment without silica. Addition of silica did not alleviate the lead release in water. Also, as mentioned previously, the lead concentration is still higher than the expected dissolved lead concentration according to the solubility of hydrocerussite (Figure 1-2). According to the calculation done by *MINEQL+*, ionic strength of synthesized Buffalo water is around

0.00756M so that at pH 7.7, predicted dissolved lead concentration would be 86 $\mu\text{g/L}$ in the system. The experimental data at pH 7.7 is sometimes higher than this level, but at pH 8.8, the predicted concentration would be 52 $\mu\text{g/L}$, which is still much lower than that in the experiments. Second, all the solubility constants, dissociation constants and stability constants are standard constants at 25°C, so the difference between real experimental condition and standard condition will result in the uncertainty of those constants and affect the accuracy of predicted concentration consequently.

During the pre-equilibrium experiment at pH 7.7 without silica, the aluminum concentration increased within 24 hours to 250 $\mu\text{g/L}$. Soon after the addition of silica, the aluminum concentration initially decreased to 170 $\mu\text{g/L}$ in the first four hours and then began to fluctuate in the range of 200-250 $\mu\text{g/L}$ with time. According to the solubility curve (Figure 1-3), the expected aluminum concentration is determined by the solubility of gibbsite (crystalline) and amorphous aluminum hydroxide. The observed concentration of aluminum is within the range of predicted dissolved aluminum. As the unidentified broad peaks in the XRD pattern of Buffalo scales were much weaker than peaks of hydrocerussite, the aluminum-contained components in the scales may contain both gibbsite and amorphous aluminum hydroxide. Therefore, the expected concentration of aluminum will have a large range and will be difficult to estimate.

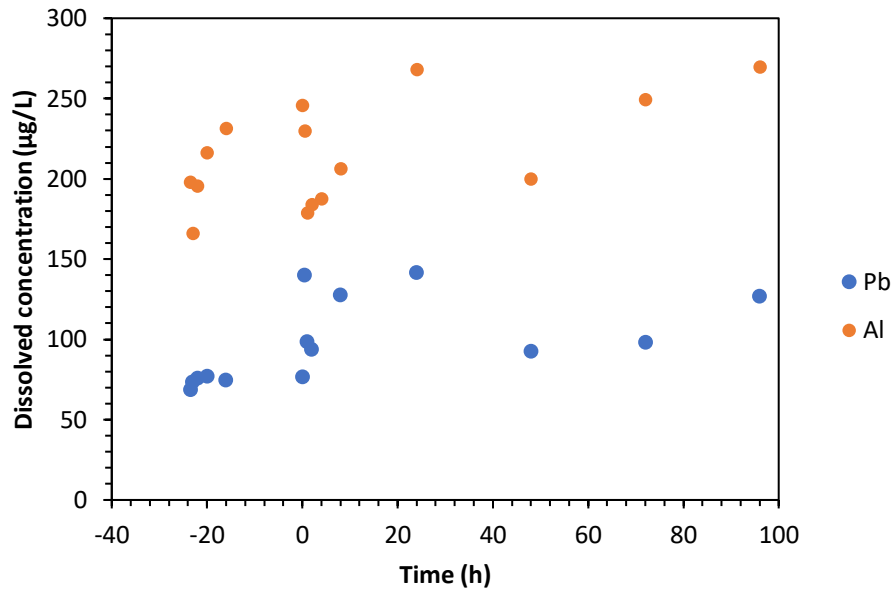


Figure 3-22: Lead and aluminum concentration variation with time at pH 7.7 (with 0.1 g scales and 20 mg/L silica in 50 mL of solution)

At pH 8.8, after the addition of silica and pH adjustment in the reactor, the lead concentration began to fluctuate around 100 µg/L, which remained the same as that before the addition of silica. The aluminum concentration began to fluctuate in the range of 400-600 µg/L. The measured lead concentration is still higher than the expected dissolved lead concentration according to the solubility of hydrocerussite, while the aluminum concentration is in the range of expected dissolved aluminum concentration.

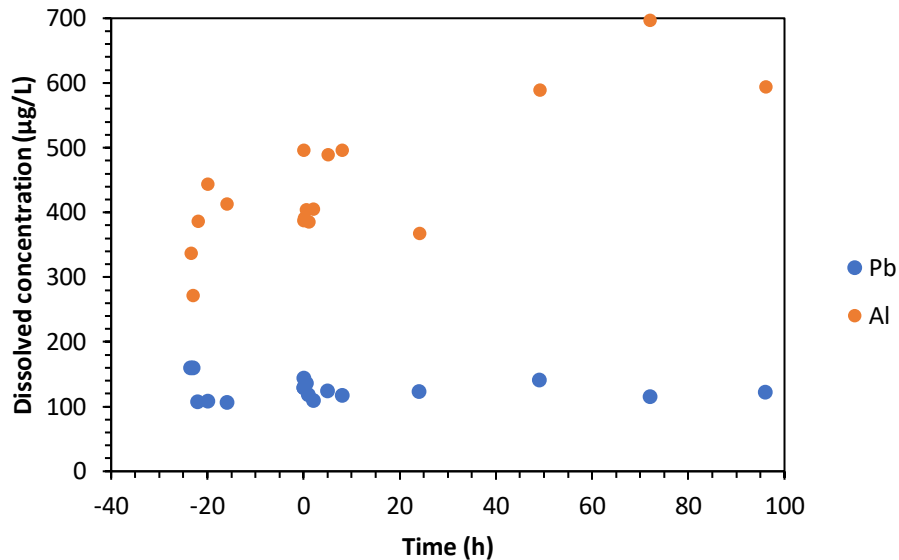


Figure 3-23: Lead and aluminum concentration variation with time at pH 8.8 (with 0.1 g scales and 20 mg/L silica in 50 mL of solution)

In both figures above, a decrease in the aluminum concentration occurs as soon as silica is added to the system. The dissolved aluminum is interacting with the added silica, which could involve the precipitation of some amorphous aluminosilicate solid.

In both types of batch experiments (pure hydrocerussite and powdered scale), the addition of sodium silicate did not decrease lead release to the water, but the addition of sodium silicates to pipe loops that had the similar pipes to those from which the scale was extracted did result in decreased release of lead to the water. These different observations for powdered scale and intact scale on a pipe are probably due to the ways in which the silica interacts with the intact scales to control the transport of lead from the lead pipe surface through the scale to the water. For the powdered scales, the large surface area and grinding of the scales probably made the lead-rich portions of the powdered material easily accessible to the well-mixed water. In contrast for the pipes with the intact scales, the most lead-rich portions of the scale are physically separated from the water by a lead-poor layer of scale.

Chapter 4

Conclusions and Recommendations for Future Work

4.1 Conclusions

Based on the batch experiments of silica uptake by pure hydrocerussite and scales extracted from lead service lines, we can propose several processes for the uptake of silica by these materials. One of the main reasons for the uptake of silica can be attributed to the adsorption of silica by hydrocerussite and scales. The other reason can be the interactions taking place between the dissolved silica species and solids. Precipitation of silica with hydrocerussite or aluminum hydroxide in the solution is another important process which can reduce the silica concentration in the solution. The formation of polymeric silica in solution (5-10%) when sodium silicate is added can reduce the total monomeric species detected and result in higher silica loss from the water than actually lost. Formation of polymeric silica is enhanced at elevated pH as we can see in Table 1-1. In Figure 3-3 we can see that in the isotherm, sorption density is not reaching a plateau as the equilibrium concentration of silica increases. A possible explanation for this phenomenon is that after the uptake of silica by solids the silica starts to convert into polymeric silicate.

The biphasic model successfully fits the experimental data for the rate of silica uptake by both hydrocerussite and scales. The total reaction time is divided into a fast uptake stage and a slow uptake stage. The fast stage could be the result of the uptake of silica by solids and the slow stage is the result of formation of polymeric silicate uptake. In the comparison of the rates of silica uptake by hydrocerussite and by scales, both have a rapid stage and a slower stage. If we compare the two reaction constants in the biphasic model of both hydrocerussite and scales, we can see that k_1 and k_2 for both adsorbents are quite close at pH 8.8. At pH 7.7, the rate constant k_2 is close to that of both adsorbents at pH 8.8, while k_1 is higher than that at pH 8.8, which indicates that pH will also affect the rate constant of the uptake of dissolved silica. This assumption is quite reasonable because the concentrations of different silica species are affected by pH value. Therefore, this hypothesis explains the

slow stage with similar rate constants existing in both hydrocerussite case and scale case, and the difference of uptake rate in the rapid stage at different pH values. In conclusion, the fast stage could be caused by some rapid chemical reactions (adsorption and polymerization to form a precipitate) on the exterior surface of the adsorbent particles, and the slow stage could be caused by a slow reaction, say, the conversion of monomeric silica into polymeric silica.

The study in this thesis is basically focusing on the uptake of silica, but from the variation of metal concentration with time we can see that the addition of silica was not controlling the release of lead as it did in the associated pipe loop system. The scales used in batch experiments were completely ground to powder and were contained in plastic reactors thereby eliminating loss of silica by mass transfer.

4.2 Recommendations for Future Work

4.2.1 Suggestions for Experiments

More experiments with different masses of scales and initial dissolved silica concentrations will help in building an isotherm for sorption of silica onto scales. Due to the fact that monomeric silica will convert into polymeric in a solution, the method of measuring dissolved silica concentration can be updated. The colorimetric method mentioned in Chapter 2 can still be applied to measure monomeric silica whereas an updated method mentioned in *Standard Methods for the Examination of Water and Wastewater* can be used to measure total silica. The polymeric silica can be calculated to estimate the actual silica uptake. In the Buffalo water chemistry (Table 1-5), 48 mg/L of calcium was added, which has a great chance to form compounds containing calcium and silica. Therefore, using ICP-OES to measure calcium concentration in the reactors can determine the change in concentration of calcium during silica uptake. Based on the XRD pattern, the bulk of the scale is assumed to be amorphous in nature because any changes in the scale characteristics cannot be observed. NMR or FTIR analysis of solids before and after the reactions could be

used to gain helpful insights into the bonds formed and broken during the reactions. Additionally, it would be useful to measure zeta potentials of the hydrocerussite and powdered scale particles before and after sodium silicate addition.

As shown in the acid digestion result, Buffalo scales mainly contain lead-based and aluminum-based solid phases. Research mentioned in the review of relevant literature about interactions between dissolved silica and aluminum minerals (like aluminum hydroxide) could be repeated to further support and demonstrate results in this study.

4.2.2 Suggestions for Improvements of Modeling

It is reported that the adsorption of silica can be modeled using a surface complexation model ^[29], the same method might be feasible for silica uptake by scales. Therefore, quantitative experiments carried out within a broader range of pH values could be done to develop a surface complexation model.

References

- [1] Rudolph, A. M.; Rudolph, C. D., Hostetter, M. K. et al. 2003. "Lead". Rudolph's Pediatrics (21st ed.). McGraw-Hill Professional. p. 369.
- [2] World Health Organization. 2011. *Guidelines for Drinking-water Quality*.
- [3] U.S.EPA, 1991. Maximum contaminant level Goals and national primary drinking water regulations for lead and copper. Final Rule. Federal Register 56, 26460.
- [4] Environmental Protection Agency, 2019. LCR Proposal Summary and Key Improvements.
- [5] Mishrra, A., Giammar, D., 2019. Effects of Sodium Silicate Corrosion Inhibitors on Lead Release from Pipe Materials. Abstracts of Papers of the American Chemical Society 257.
- [6] Thresh, J.C. (1922). The Action of Natural Waters on Lead. Analyst, 47, 500-505.
- [7] Lytle, D.A., Schock, M.R., 2000. Impact of stagnation time on metal dissolution from plumbing materials in drinking water. Journal of Water Supply Research and Technology-Aqua 49 (5), 243-257.
- [8] Schock, M.R., 1989. Understanding corrosion control strategies for lead. Journal American Water Works Association 81 (7), 88-100.
- [9] Schock, M.R., 1999. In: Letterman, R.D. (Ed.), Water Quality and Treatment. McGraw-Hill, Inc., New York, New York.
- [10] Kim, E.J., Herrera, J.E., Huggins, D., Braam, J., Koshowski, S., 2011. Effect of pH on the concentrations of lead and trace contaminants in drinking water: a combined batch, pipe loop and sentinel home study. Water Research 45 (9), 2763-2774.
- [11] Nawrocki, J., Raczyk-Stanislawiak, U., Swietlik, J., Olejnik, A., Sroka, M.J., 2010. Corrosion in a distribution system: steady water and its composition. Water Research 44 (6), 1863-1872.
- [12] Environmental Protection Agency, 1992. Lead and Copper Rule Guidance Manual. Vol. 2, 3-17.

- [13] Thompson, J. L., Scheetz, B. E., Schock, M. R., & Lytle, D. A. (1967). Sodium Silicate Corrosion Inhibitors: Issues of Effectiveness and Mechanism. *Corrosion*, 1(3), 221-227.
- [14] Thompson, J.L., Scheetz, B.E., Schock, M.R., Lytle, D.A., and Delaney, P.J. (1997) Sodium silicate corrosion inhibitors: issues of effectiveness and mechanism, Proc. AWWA Water Quality Technology Conference, Denver, CO.
- [15] AWWARF. (1996). Internal Corrosion of Water Distribution Systems, Second Edition.
- [16] Lehrman, L., & Shuldener, H. L. (1951). The Role of Sodium Silicate in Inhibiting Corrosion by Film Formation on Water Piping. *Journal - American Water Works Association*, 43(3), 175-188.
- [17] Duffek, E. F., & McKinney, D. S. (1956). New Method of Studying Corrosion Inhibition of Iron with Sodium Silicate. *Journal of The Electrochemical Society*, 103(12), 645-648.
- [18] Jackson, P.J., Sheiham, I. (1980). Calculation of lead solubility in water. Water Research Centre Technical Report, TR-152.
- [19] Michniewicz, D.C., J.A. Clement, T.S. Gimpel, and M.S. Schock (1993). Sodium Silicate for the Simultaneous Control of Lead, Copper and Iron Based Corrosion. Report on York Water District, York, ME.
- [20] Schantz, L.G. (1994). Summary of Corrosion Control Studies. Report by the City of Rochester, Rochester Water Bureau, Water Quality Operations, Rochester, NY
- [21] Luxton, T. P., Eick, M. J., & Rimstidt, D. J. (2008). The role of silicate in the adsorption/ desorption of arsenite on goethite. 252, 125–135.
- [22] Maiti, A., Basu, J. K., & De, S. (2012). Experimental and kinetic modeling of As(V) and As(III) adsorption on treated laterite using synthetic and contaminated groundwater: Effects of phosphate, silicate and carbonate ions. *Chemical Engineering Journal*, 191, 1–12.
- [23] Meng, X., Bang, S., & M, G. P. K. (2000). Effects of silicate, sulfate, and carbonate on arsenic removal by ferric chloride. 34(4).
- [24] Tokoro, C., Suzuki, S., Haraguchi, D., & Izawa, S. (2014). Silicate Removal in Aluminum Hydroxide Co-Precipitation Process. (ii), 1084–1096.

- [25] Baird, R., Eaton, A., Rice, E., Bridgewater, L. (2017). *Standard Methods for the Examination of Water and Wastewater*, 23rd Edition.
- [26] Pan, W., Pan, C., Bae, Y., Giammar, D. (2019). Role of Manganese in Accelerating the Oxidation of Pb(II) Carbonate Solids to Pb(IV) Oxide at Drinking Water Conditions. *Environmental Science & Technology*, 53(Ii), 6699–6707.
- [27] Kushnir, C. (2014). Influence of Water Chemistry Parameters on the Dissolution Rate of the Lead(II) Carbonate Hydrocerussite.
- [28] Noel, J. D., Wang, Y., Giammar, D. E. (2014). ScienceDirect Effect of water chemistry on the dissolution rate of the lead corrosion product hydrocerussite. *Water Research*, 54, 237–246.
- [29] Jolsterå, R., Gunneriusson, L., & Forsling, W. (2010). Journal of Colloid and Interface Science Adsorption and surface complex modeling of silicates on maghemite in aqueous suspensions. *Journal of Colloid and Interface Science*, 342(2), 493–498.
- [30] Davis, J.A. and Kent, D.B. (1990). *Mineral-Water Interface Geochemistry*. Reviews in Mineralogy & Geochemistry, Vol. 23.
- [31] Davis, C. C., & Chen, H. (2002). Modeling Silica Sorption to Iron Hydroxide. *Environmental Science & Technology*, 36(4), 582–587.

Appendices

A. The Constants Used in the Calculation of Aquatic Chemistry

Table S1. Chemical formulas and acidity constants at 25°C of some important acids

Chemical	Formula	pK _{a1}	pK _{a2}	pK _{a3}
Hydrochloric acid	HCl	<0		
Sulfuric acid	H ₂ SO ₄	<0	1.99	
Hydronium ion	H ₃ O ⁺	0.00	14.00	
Phosphoric acid	H ₃ PO ₄	2.148	7.198	12.375
Hydrofluoric acid	HF	3.18		
Carbonic acid	H ₂ CO ₃	6.352	10.329	
Hypochlorous acid	HOCl	7.53		

Table S2. Stability constants for some Al-ligand and Pb-ligand complexes. Values correspond to logβ for formation of the complex.

	OH ⁻		CO ₃ ²⁻		SO ₄ ²⁻		Cl ⁻		F ⁻		PO ₄ ³⁻
AlL	9.00			AlL	3.84	AlL	-0.39	AlL	7.01	AlHL	20.01
AlL ₂	17.71			AlL ₂	5.58			AlL ₂	12.63	Al ₂ L	18.98
AlL ₃	25.31							AlL ₃	16.70		
AlL ₄	33.00							AlL ₄	19.40		
PbL	6.40	PbL	6.53	PbL	2.69	PbL	1.56	PbL	2.15	PbHL	15.48
PbL ₂	10.91	PbL ₂	9.94	PbL ₂	3.47	PbL ₂	1.90	PbL ₂	3.24	PbH ₂ L	21.07
PbL ₃	13.91	PbHL	13.23			PbL ₃	1.80				
						PbL ₄	1.38				

Table S3. The K_{s0} value of some solids of interest

Metal	Mineral	Formula	log K _{s0}
Al ³⁺	Amorphous Aluminum Hydroxide	Al(OH) ₃	-31.20
Al ³⁺	Gibbsite	Al(OH) ₃	-34.26
Pb ²⁺	Hydrocerussite	Pb ₃ (CO ₃) ₂ (OH) ₂	-46.76
Pb ²⁺	Cerussite	PbCO ₃	-13.20

B. The Calculation of Solubility Curves

a. Dissolved Lead Concentration

$$\begin{aligned}
 [Pb]_{diss} &= [Pb^{2+}] + [Pb(OH) - sum] + [Pb(CO_3) - sum] \\
 &\quad + [other\ negligible\ complexations] \\
 &= [Pb^{2+}] + [Pb(OH)^+] + [Pb(OH)_2^0] + [Pb(OH)_3^-] + [PbCO_3^0] + [Pb(CO_3)_2^{2-}] \\
 &\quad + [PbHCO_3^+] \\
 &= [Pb^{2+}](1 + \beta_1[OH^-] + \beta_2[OH^-]^2 + \beta_3[OH^-]^3 + K_{PbL}[CO_3^{2-}] \\
 &\quad + K_{PbL_2}[CO_3^{2-}]^2 + K_{PbHL}[H^+][CO_3^{2-}]) \\
 [CO_3^{2-}] &= \frac{TOTCO_3}{\frac{[H^+]^2}{K_{a1}K_{a2}} + \frac{[H^+]}{K_{a2}} + 1}, K_{a1} = 10^{-6.35}, K_{a2} = 10^{-10.33}. \\
 K_{sp}(Pb_3(OH)_2(CO_3)_2) &= [Pb^{2+}]^3[OH^-]^2[CO_3^{2-}]^2 = 10^{-46.76}
 \end{aligned}$$

b. Dissolved Aluminum Concentration

$$\begin{aligned}
 [Al]_{diss} &= [Al^{3+}] + [Al(OH) - sum] + [Al(SO_4) - sum] + [Al(F) - sum] + [Al(PO_4) \\
 &\quad - sum] + [other\ negligible\ complexations] \\
 &= [Al^{3+}] + [Al(OH)^{2+}] + [Al(OH)_2^+] + [Al(OH)_3^0] + [Al(OH)_4^-] + [Al(SO_4)^+] \\
 &\quad + [Al(SO_4)_2^-] + [AlF^{2+}] + [AlF_2^+] + [AlF_3^0] + [AlF_4^-] + [AlHPO_4^+] \\
 &\quad + [Al_2PO_4^{3+}] \\
 &= [Al^{3+}](1 + \beta_1[OH^-] + \beta_2[OH^-]^2 + \beta_3[OH^-]^3 + \beta_4[OH^-]^4 + \beta_{AlSO_4_1}[SO_4^{2-}] \\
 &\quad + \beta_{AlSO_4_2}[SO_4^{2-}]^2 + \beta_{AlF_1}[F^-] + \beta_{AlF_2}[F^-]^2 + \beta_{AlF_3}[F^-]^3 + \beta_{AlF_4}[F^-]^4 \\
 &\quad + \beta_{AlHPO_4}[H^+][PO_4^{3-}] + \beta_{Al_2PO_4}[Al^{3+}][PO_4^{3-}]) \\
 [PO_4^{3-}] &= \frac{TOTPO_4}{\frac{[H^+]^3}{K_{a1}K_{a2}K_{a3}} + \frac{[H^+]^2}{K_{a2}K_{a3}} + \frac{[H^+]}{K_{a3}} + 1} \\
 K_{a1} &= 10^{-2.148}, K_{a2} = 10^{-7.198}, K_{a3} = 10^{-12.375}
 \end{aligned}$$

$$[SO_4^{2-}] = \frac{K_{a2}TOTSO_4}{K_{a2} + [H^+]}, K_{a2} = 10^{-1.99}$$

$$[F^-] = \frac{K_aTOTF}{K_a + [H^+]}, K_a = 10^{-3.18}$$

$$K_{sp}(Al(OH)_3(amorphous)) = [Al^{3+}][OH^-]^3 = 10^{-31.20}$$

$$K_{sp}(Al(OH)_3(gibbsite)) = [Al^{3+}][OH^-]^3 = 10^{-34.26}$$

C. Calibration Curves Used in the Experiments

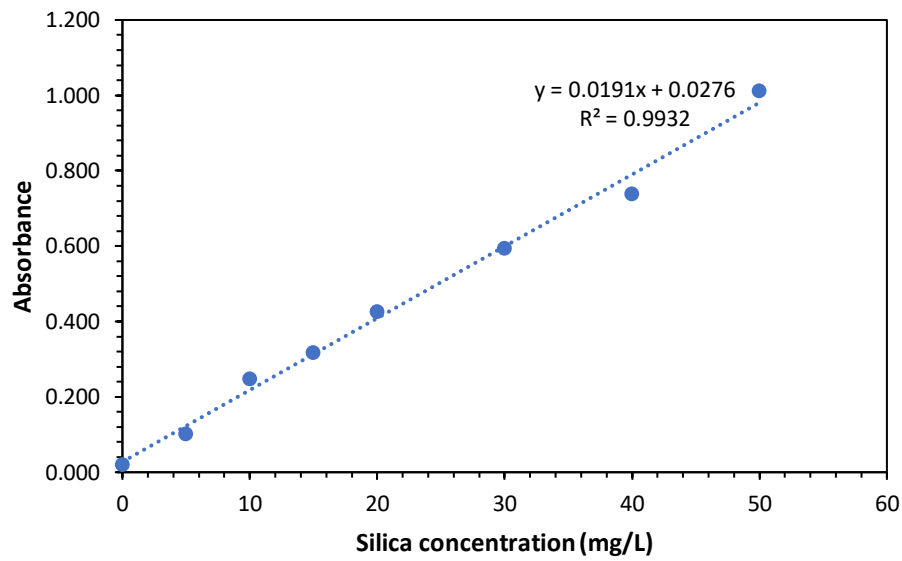


Figure S1. Calibration curve of silica (UV-Vis wavelength $\lambda=410$ nm)

Table S4. Standard silica concentration calibration

Concentration (mg/L)	Absorbance			Average abs
0	0.021	0.022	0.020	0.021
5	0.102	0.103	0.102	0.102
10	0.250	0.248	0.247	0.248
15	0.325	0.316	0.310	0.317
20	0.433	0.426	0.419	0.426
30	0.595	0.600	0.590	0.595
40	0.739	0.737	0.741	0.739
50	1.016	1.011	1.009	1.012

D. Source and Purity of Chemicals and Reagents Used in the Experiments**Table S5. Chemicals and reagents in the experiments**

Reagent	Supplier and purity
Ammonium molybdate	
Blended phosphate	Carus Corporation 70/30 blend of poly/ortho-phosphate
Calcium chloride	99-105%, Alfa-Aesar, MA
Calcium hydroxide	
Deionized water	Resistivity>18.2 MΩ-cm, Milli-Q, Millipore Corp., Milford, MA
Free chlorine (NaOCl)	5.65–6%, Fisher Scientific, NJ
Hydrocerussite	Sigma-Aldrich
Hydrochloric acid	
Nitric acid	68.0-70.0%, Alfa-Aesar, MA or Fisher Scientific (trace metal grade), NJ
Oxalic acid	
Sodium bicarbonate	≥99.7%, Sigma-Aldrich, Saint Louis, MO
Sodium fluoride	≥99%, Sigma-Aldrich, Saint Louis, MO
Sodium hydroxide	NaOH, ≥98%, Sigma-Aldrich, Saint Louis, MO
Sodium silicate (NaO:SiO ₂ =1:3.22)	PQ Corporation, n.d.
Sulfuric acid	

E. Additional Experimental Data

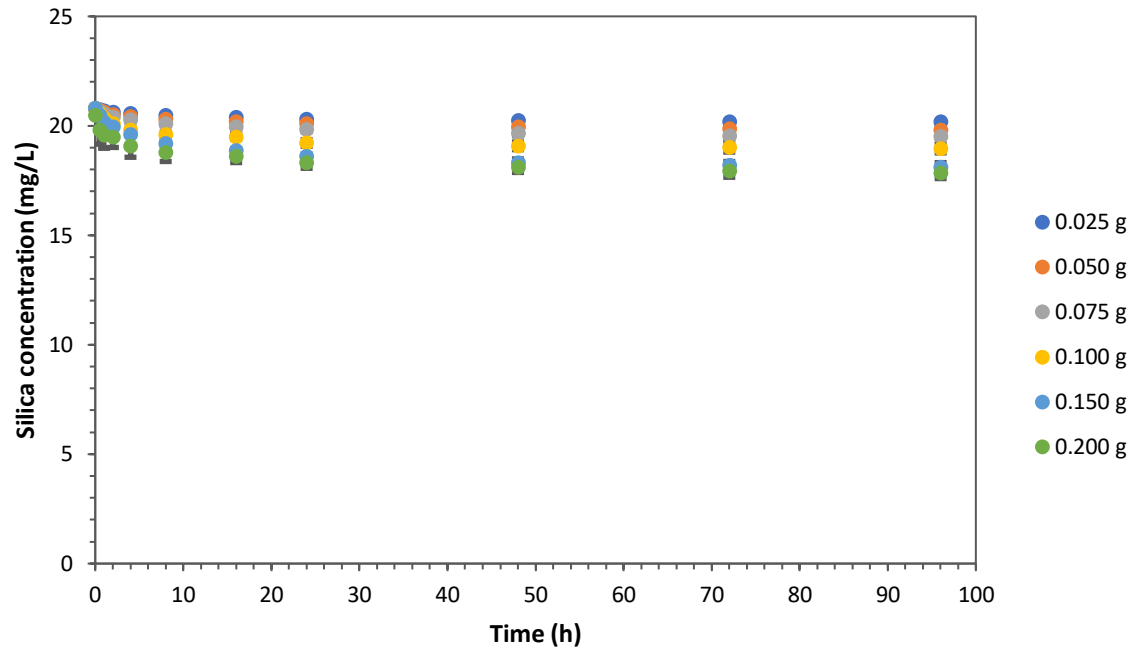


Figure S2. Silica concentration variation with time for different amounts of hydrocerussite (in 100 mL of water, initial silica concentration 20 mg/L, pH 8.8)

Vita

Ziqi Wang

Date of Birth	Aug 6, 1996
Place of Birth	Harbin, Heilongjiang, China
Degrees	B. S. Chemistry Nankai University, May 2018

May 2020

Interactions between Lead Pipe Scales and Dissolved Silica, Wang, M.S. 2020